Current trends in material research for nuclear batteries

Harnessing metal perovskite halides and other chalcogenides for greater compactness and efficiency

Kowal, D.; Mahato, S.; Makowski, M.; Hartati, S.; Sheikh, M. A.K.; Ye, W.; Schaart, D. R.; Arramel, A.; Birowosuto, M. D.; More Authors

DOI
10.1063/5.0236524

Publication date
2025

Document Version
Final published version

Published in
Applied Physics Reviews

Citation (APA)
Kowal, D., Mahato, S., Makowski, M., Hartati, S., Sheikh, M. A. K., Ye, W., Schaart, D. R., Arramel, A., Birowosuto, M. D., & More Authors (2025). Current trends in material research for nuclear batteries: Harnessing metal perovskite halides and other chalcogenides for greater compactness and efficiency. *Applied Physics Reviews*, *12*(1), Article 011328. https://doi.org/10.1063/5.0236524

Applied Physics Reviews

REVIEW ARTICLE | MARCH 12 2025

Current trends in material research for nuclear batteries: Harnessing metal perovskite halides and other chalcogenides for greater compactness and efficiency

Special Collection: Frontiers in energy materials research: novel measurement, modelling and processing approaches

D. Kowal ✉ ; S. Mahato ; M. Makowski ; S. Hartati ; M. A. K. Sheikh ; W. Ye ; D. R. Schaart ; J. Cybinska ; L. J. Wong ; A. Arramel ✉ ; M. D. Birowosuto ✉

Appl. Phys. Rev. 12, 011328 (2025)
https://doi.org/10.1063/5.0236524

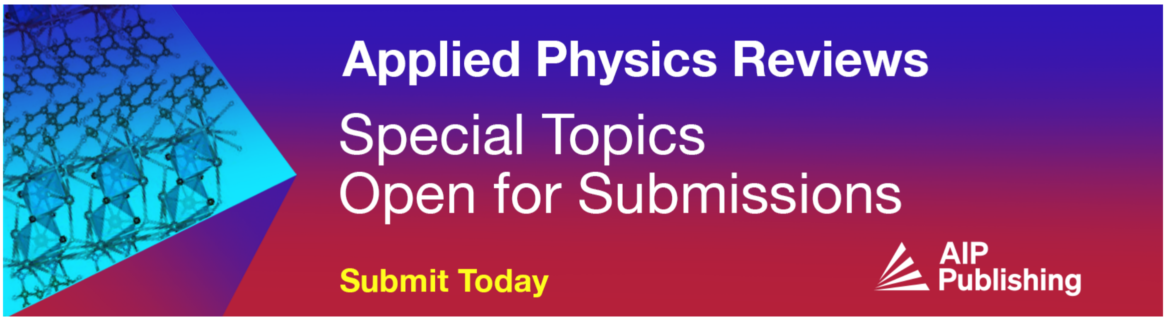

AIP Publishing

Applied Physics Reviews REVIEW pubs.aip.org/aip/are

Current trends in material research for nuclear batteries: Harnessing metal perovskite halides and other chalcogenides for greater compactness and efficiency

Cite as: Appl. Phys. Rev. **12**, 011328 (2025); doi: 10.1063/5.0236524
Submitted: 1 September 2024 · Accepted: 11 February 2025 ·
Published Online: 12 March 2025

D. Kowal,[1,a)] S. Mahato,[1] M. Makowski,[1] S. Hartati,[2] M. A. K. Sheikh,[1] W. Ye,[3] D. R. Schaart,[4] J. Cybinska,[1,5] L. J. Wong,[3] A. Arramel,[2,a)] and M. D. Birowosuto[1,a)]

AFFILIATIONS

[1] Lukasiewicz Research Network – PORT Polish Center for Technology Development, Wroclaw 54-066, Poland
[2] Center of Excellence Applied Physics and Chemistry, Nano Center Indonesia, Tangerang Selatan 15314, Indonesia
[3] School of Electrical and Electronic Engineering, Nanyang Technological University, Singapore 639798, Singapore
[4] Faculty of Applied Sciences, Department of Radiation Science and Technology, Delft University of Technology, Delft 2629 JB, Netherlands
[5] Faculty of Chemistry, University of Wroclaw, Wroclaw 50-300, Poland

Note: This paper is part of the APR Special Topic on Frontiers in energy materials research: novel measurement, modelling and processing approaches.

[a)] **Authors to whom correspondence should be addressed:** dominik.kowal@port.lukasiewicz.gov.pl; arramel@nano.or.id; and muhammad.birowosuto@port.lukasiewicz.gov.pl

ABSTRACT

Nuclear energy emerges as a promising and environmentally friendly solution to counter the escalating levels of greenhouse gases resulting from excessive fossil fuel usage. Essential to harnessing this energy are nuclear batteries, devices designed to generate electric power by capturing the energy emitted during nuclear decay, including α or β particles and γ radiation. The allure of nuclear batteries lies in their potential for extended lifespan, high energy density, and adaptability in harsh environments where refueling or battery replacement may not be feasible. In this review, we narrow our focus to nuclear batteries utilizing non-thermal converters such as α- or β-voltaics, as well as those employing scintillation intermediates. Recent advancements in state-of-the-art direct radiation detectors and scintillators based on metal perovskite halides (MPHs) and chalcogenides (MCs) are compared to traditional detectors based on silicon and III-V materials, and scintillators based on inorganic lanthanide crystals. Notable achievements in MPH and MC detectors and scintillators, such as nano-Gy sensitivity, 100 photons/keV light yield, and radiation hardness, are highlighted. Additionally, limitations including energy conversion efficiency, power density, and shelf-life due to radiation damage in detectors and scintillators are discussed. Leveraging novel MPH and MC materials has the potential to propel nuclear batteries from their current size and power limitations to miniaturization, heightened efficiency, and increased power density. Furthermore, exploring niche applications for nuclear batteries beyond wireless sensors, low-power electronics, oil well monitoring, and medical fields presents enticing opportunities for future research and development.

TABLE OF CONTENTS

I. INTRODUCTION

Nuclear energy is increasingly recognized as an essential component of global efforts to reduce greenhouse gas emissions and combat climate change. An innovative application of nuclear energy is the development of nuclear batteries that directly convert energy into electricity.[1] These batteries utilize energy released during the decay of radioactive isotopes, including α and β particles and γ radiation. The potential advantages of nuclear batteries are significant, such as long-life expectancy, high energy density, and the ability to work in environments where conventional batteries are not easily replaced or recharged.[2] Nuclear batteries are widely used in various sectors. In space exploration, they provide a reliable power source that is resistant to harsh conditions in space and helps to carry out long missions without the need for frequent maintenance. In addition, in the fields of defense, industrial drilling, medicine, electronics, and research, these batteries improve the performance of devices; provide longevity, safety, and compactness; and thus revolutionize technology in various fields.[1–3] As a result, the market for nuclear batteries is expected to reach US$ 103.22 billion by 2029, with a compound annual growth rate (CAGR) of 8.8% in the forecast period. For micro-watt batteries, more research is required before they are ready for the market.[4,5]

Nuclear batteries can be broadly classified into thermal converters and non-thermal converters.[1] Non-thermal converters directly use the motion energy of nuclear decay particles to produce electricity without heat dependence, which offers efficiency and compactness advantages.[2] Historically, these devices used silicon and III-V semiconductors, but recent advances have highlighted the superior performance of metal perovskite halides (MPHs)[6] and metal chalcogenides (MCs).[7,8] Recent scintillator-based systems that rely on MPHs[9–11] and MCs[12–14] that convert high-energy radiation into visible light and convert them into photodetectors are especially useful for capturing γ radiation and provide the potential for longer battery life.

There are not so many reviews focused on the latest trends in nuclear battery materials research,[1–3] in particular the use of MPHs and MCs. These materials are very promising in improving the performance of nuclear batteries through direct and indirect energy conversion methods. Recent research has shown that MPHs are known for their remarkable optical and electronic properties, while MCs are well stable and resistant to radiation, setting new standards for radiation detection and energy conversion.[6–8] In the future, this will be a first-class development of smaller, more efficient, and powerful nuclear batteries.

Recent research has shown that MPHs and MCs offer significant improvements over traditional materials used in radiation detections.[6–8] Among the notable achievements of these materials are the sensitivity of nano-Gy, which improves the detection of low radiation; the high light output of 100 000 photons per MeV (ph/MeV), which is crucial for efficient scintillation; and the superior radiation hardness, which allows these materials to maintain their performance in high radiation environments. These advances are leading to the development of smaller, more efficient, and more powerful nuclear batteries for MPH and MC.

Despite these promising developments, several challenges remain. The key areas that need to be further explored include improvement of power conversion efficiency (PCE) and energy density, improvement of material longevity and radiation resistance, and miniaturization of nuclear batteries without compromising their energy output.[6–8] These challenges represent exciting opportunities for further innovations in this field. With the progress of research, the potential applications of advanced nuclear batteries can extend beyond current applications of wireless sensors, low-power electronics and medical devices to space exploration, remote sensing, and advanced medical treatments.[1–3]

The review is organized as follows: an overview of nuclear batteries with an emphasis on non-thermal converters; an explanation of the properties and properties of different radioisotopes; an explanation of the α, β, and γ energy conversion mechanisms; an overview of current technologies and materials, including silicon carbide, III-V semiconductors, and emerging nanocomposites; an overview of nuclear batteries based on scintillators and their development status; and an analysis of MPHs in direct detection and scintillation in these areas. The aim of this review is to provide a comprehensive understanding of current trends and future prospects in nuclear battery material research and to highlight the potential for the transformation of MPHs and metal chalcogenides in this field.

II. GENERAL CONCEPT OF NUCLEAR BATTERIES

Nuclear batteries are designed to transform the energy carried by high energy radiation emitted by chosen radioisotope into electricity. This is either achieved using thermal conversion, based on thermoelectric effect in the radiation absorber, or through non-thermal conversion scheme, sometimes referred to as "radiovoltaic" as analogy to photovoltaic (PV) devices that are based on charge carrier generation in semiconducting heterostructures following the absorption of light. In this review, we mostly focus on the non-thermal detection schemes and discuss the potential of some novel nuclear battery designs by making the link to unique optoelectronic properties of MPHs and MCs. Additionally, we note that the thermal conversion technology can benefit in future from the use of novel types of MCs with remarkable thermoelectric behavior.

A. Suitable radioisotopes for nuclear batteries

Table I presents a comparison of isotopes with possible application in nuclear batteries, with primary radiation type of the source, half-life, emitted radiation energy, power density (PD)[15] as well as other relevant features. The PD of a radioactive source is crucial for nuclear batteries. It directly influences the battery's efficiency, size,

TABLE I. Comparison of selected isotopes. Value of power density was calculated with an assumption of maximum value achievable for 1 g of pure isotope of each radiation source and area of 1 cm^2. Data taken from online database.[15]

Isotope	Radiation type	Half-life	Energy (keV)	Pow. den. (W/cm^2)	γ (keV)	Heat generation	Decay product toxicity
Curium-242 (^{242}Cm)	α	162.8 D	6216	122	44	Significant	Toxic (^{238}Pu)
Curium-244 (^{244}Cm)	α	18.1 y	5902	2.83	43	Significant	Toxic (^{240}Pu)
Americium-241 (^{241}Am)	α	432 y	5638	0.11	59.5	Moderate	Toxic (^{237}Np)
Plutonium-238 (^{238}Pu)	α	87.7 y	5593	0.57	43.5	Significant	Toxic (^{234}U)
Polonium-210 (^{210}Po)	α	138.4 D	5408	144	···	Significant	Toxic (^{206}Pb)
Radium-226 (^{226}Ra)	α	1600 y	4870	0.03	186	Moderate	Toxic (^{222}Rn)
Uranium-238 (^{238}U)	α	4.47×10^9 y	4198	8.3×10^{-9}	···	Moderate	Toxic (^{234}Th)
Krypton-85 (^{85}Kr)	β	10.8 y	681	1.60	514	Negligible	Toxic (^{85}Rb)
Cesium-137 (^{137}Cs)	γ	30.2 y	662	0.32	···	Moderate	Toxic (^{137}Ba)
Strontium-90 (^{90}Sr)	β	28.8 y	546	0.46	···	Moderate	Toxic (^{90}Y)
Cobalt-60 (^{60}Co)	β	5.27 y	318	2.14	1200	Minimal	Toxic (^{60}Ni)
Technetium-99 (^{99}Tc)	β	2.1×10^5 y	294	2.92×10^{-5}	···	Negligible	Low-toxic (^{99}Ru)
Promethium-147 (^{147}Pm)	β	2.62 y	224	1.25	121	Negligible	Toxic (^{147}Sm)
Sulfur-35 (^{35}S)	β	87.4 D	167	42.2	···	Minimal	Non-toxic (^{35}Cl)
Carbon-14 (^{14}C)	β	5730 y	156	4.12	···	Negligible	Non-toxic (^{14}N)
Nickel-63 (^{63}Ni)	β	100 y	66.9	3.96	···	Minimal	Non-toxic (^{63}Cu)
Ruthenium-106 (^{106}Ru)	β	1 y	39	0.78	512	Moderate	Toxic (^{106}Rh)
Tritium (^{3}H)	β	12.3 y	18.6	0.70	···	Negligible	Non-toxic (^{3}He)

weight, and suitability for various applications. It is calculated using formula:

$$PD = E \times \Phi / A, \tag{1}$$

where E, Φ, and A stand for the emitted radiation energy in Joules, flux (number of particles emitted over a period), and area through which the radiation passes (in cm^2), respectively. Another parameter of interest when selecting a source for specific application is the type of radioactive decay. Each type (α, β, and γ) reveals both advantages and disadvantages. α emitters deposit a significant amount of energy over a short distance, making them efficient for ionizing materials in nuclear batteries. Due to their relatively large mass and charge, α particles are easily stopped by thin materials, reducing the need for heavy shielding. α particles are typically stopped by a few centimeters of air or a thin layer of shielding, reducing the risk of exposure to surrounding materials. The second type of radiation is β particles, which, due to smaller mass, travel with greater speed compared to α particles and penetrate materials more effectively. They have lower ionization potential and can be shielded more effectively compared to α particles. β particles deposit energy over a larger distance compared to α particles, which may affect the efficiency of energy conversion and the design of the battery. β radiation is also accompanied by the so-called Bremsstrahlung that results from deceleration or deflection of β particles (electrons or positrons) by the atomic nuclei in the surrounding material.

The extent of Bremsstrahlung radiation depends on the energy of the emitted β particles and the atomic number of the material in which the radiation is occurring. Bremsstrahlung radiation is both a challenge and an opportunity for nuclear batteries. It represents an energy loss mechanism that can reduce efficiency and requires additional shielding to manage secondary radiation. However, with innovative design strategies, it might be possible to mitigate these challenges or even harness the Bremsstrahlung radiation to enhance the performance of nuclear batteries. Since Bremsstrahlung presents certain difficulties for an early stage of nuclear batteries, it is optimal to use sources with extremely low or negligible Bremsstrahlung. In Table I, sources marked with bold font reveal high or moderately high Bremsstrahlung, which with the current state of art is considered as a negative effect. The last type of radiation is γ, which is the least ionizing form of radiation, primarily interacting with matter through electromagnetic processes, resulting in sparse ionization along their path. Due to the highest penetration depth, it requires a very thick absorber, which would negatively influence the size of a nuclear battery. However, as we discuss in further sections of this review, it is possible to exploit γ sources in radiovoltaic batteries with the help of carefully chosen scintillating materials.

In summary, once deciding on the radiation source for nuclear batteries, one has to take into consideration a plethora of parameters. First of all, higher PD value could help to scale down the battery size. Also, in the case of β particles, the mostly negative influence of bremsstrahlung must be taken into consideration, which reduces the number of applicable sources. Another factor is the number of emitted radiation energies. It is usually more convenient to work with a source that emits only one type and one energy of radiation instead of sources that are characterized by several of those. Taking these into account, the most suitable candidates would be ^{210}Po and ^{241}Am (α-particles), ^{137}Cs (γ-photons), and ^{35}S, ^{14}C, ^{63}Ni, and ^{3}H (β-particles). In the case of ^{241}Am source, the emitted γ has low energy and its contribution in an overall decay is low enough to safely handle the source. Moreover, we cannot skip a price discussion. The ^{210}Po is rare and expensive due to its scarcity and the complex process required for its production.

^{241}Am and ^{137}Cs are much more available and price friendly since they appear as a by-product of nuclear reactions. Nevertheless, for γ sources also, the price of scintillator needs to be included, which can significantly increase the price of nuclear batteries. Finally, the β-emitters seems to be the cheapest compared to other contestants since they are more common and may be produced through various methods, including nuclear reactors and particle accelerators.

There are also two additional parameters that must be considered while thinking about the applicability of such batteries in everyday life, such as heat generation and toxicity of decay products. Radiation sources with significant heat generation with highly toxic decay products would be hardly applicable since additional external cooling and proper waste disposal would make the use of such devices exceptionally suboptimal. Therefore, by taking into consideration the parameters mentioned above, ^{63}Ni and ^{3}H isotopes are the most suitable ones, which is why the commercially available nuclear batteries are typically based on those two sources. While considering ^{3}H isotope, its delivery form also has to be considered. In elevated (above cryogenic) temperatures, ^{3}H is delivered in a solid form of tritides. Tritides are metal–hydride compounds where ^{3}H binds with metals like titanium or zirconium. Concentration of ^{3}H in tritides reaches up to 66%, which further lowers the PD of such radiation source. In Table I, PD value for ^{3}H source was properly recalculated to show the real, maximum values.

B. Thermal conversion of radioactive energies

Thermal conversion of radioactive energy is a crucial aspect of nuclear battery technology, primarily achieved through radioisotope thermoelectric generators (RTGs).[16–18] These generators are efficient devices that transform heat from radioactive decay into electrical power. Central to an RTG is a robust container that houses radioactive material, or fuel, which generates heat as it decays.[1] This heat is transferred to thermocouple-components made of two different metals or semiconductors embedded in the container walls. One end of each thermocouple is connected to a heat sink, creating a temperature difference between the radioactive fuel and the cooler external environment. This temperature gradient drives the Seebeck effect, where heat is directly converted into electrical energy, and it is represented by the Seebeck coefficient as

$$S = -\Delta V/\Delta T, \tag{2}$$

where ΔV is the voltage induced by small temperature change ΔT. The varying temperatures at the junctions of the thermocouples generate an electric current. To boost voltage output, multiple thermocouples are often connected in series, making RTGs a reliable power source, particularly in space missions or remote locations where traditional energy sources are unavailable.[1]

RTGs, although effective, differ significantly from nuclear fission reactors in their operational principles. Unlike fission reactors, which use controlled nuclear reactions managed by control rods to adjust power output, RTGs rely on the constant, spontaneous decay of radioactive isotopes.[17] This decay produces heat at a steady rate that cannot be altered, leading to a gradual decline in power as the fuel depletes over time. Because RTGs cannot adjust power to meet varying demands, they often require auxiliary power sources, such as rechargeable batteries, to manage fluctuations. Additionally, continuous cooling is necessary to prevent overheating, particularly during critical stages like launch and early flight. Although RTGs are generally safe from catastrophic failures like nuclear meltdowns, they do carry risks of radioactive contamination if damaged. Therefore, although RTGs are dependable in extreme conditions, careful handling is essential to minimize potential hazards.[19]

C. Non-thermal conversion of radioactive energies

The principle of operation of radiovoltaic battery (RVB) is based on the generation and separation of charge carriers in the semiconducting heterostructure, such as PN junction[20] or Schottky diode.[21]

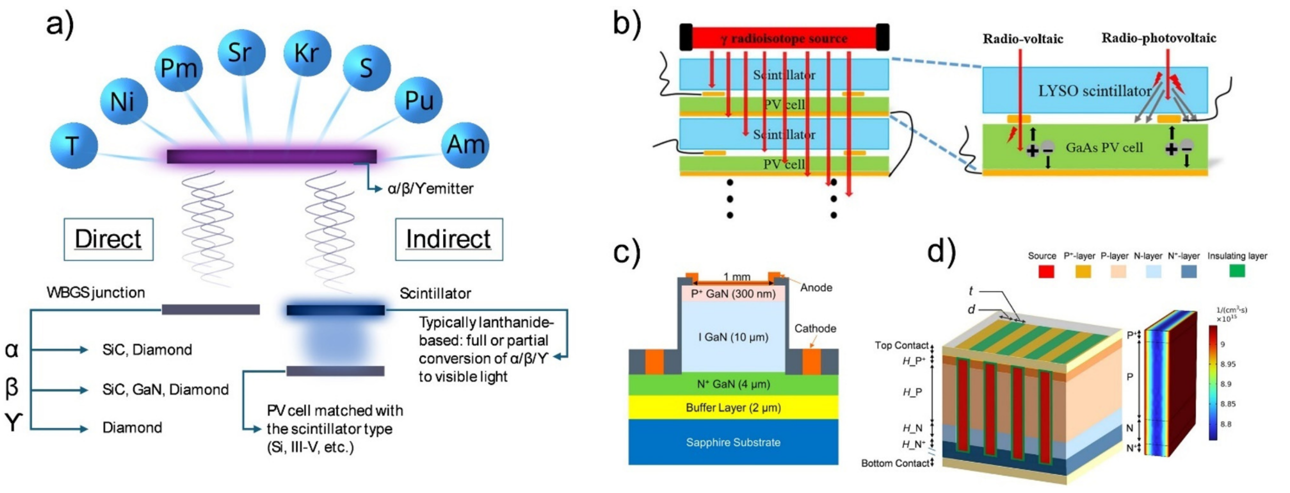

FIG. 1. General scheme of nonthermal nuclear battery architecture with some of the state-of-the-art solutions. (a) Operation principle of the device. (b) Example of γ-voltaic device with using LYSO scintillator. Reproduced with permission from Sens. Actuators A Phys. **275**, 1190129 (2018). Copyright 2018 Elsevier.[25] (c) Gallium nitride α-voltaic cell with 4.5% efficiency. Reproduced with permission from Comm. Mater. **4**, 51–58 (2023). Copyright 2023 Springer Nature.[54] (d) Example of β-voltaic device incorporating radioactive source in the PN junction. Reproduced with permission from Nucl. Sci. Tech. **34**, 180–196 (2023). Copyright 2023 Springer Nature.[70]

Figure 1(a) presents the schematic view of the RVB with some of the state-of-the-art material solutions for indirect and direct detection schemes shown in Figs. 1(b)–1(d). In direct detection scheme, the device consists of radioactive source, which is attached or incorporated into the semiconducting heterostructure, and the whole ensemble is shielded, ensuring no hazardous radiation leaks to the surroundings. Typical material choice for direct radiovoltaics is wide bandgap semiconductor (WBGS) such as SiC,[22] diamond,[23] or some III-V materials.[24] The use of WBGSs in this case is driven by their higher conversion efficiency as well as better radiation hardness, tolerance to temperature, and electric fields as compared to conventional semiconductors. Alternatively, an indirect detection scheme has been developed, which involves the use of scintillator as intermediate medium, e.g., lanthanide based crystals,[25] that serves to convert incoming radiation from radioisotope to visible/UV light. The light is then captured and converted to electricity by the conventional PV cell, such as Si- or III-V based. Devices that use such indirect schemes of operation are often referred to as radio-PV batteries (RPVBs). Most important parameter expressing the performance of RVBs and RPVBs is the PCE, which is given by

$$\mathrm{PCE} = \frac{\mathrm{P_{max}}}{\mathrm{P_{source}}} \times 100\% = \frac{\mathrm{I_{sc}} \times \mathrm{V_{oc}} \times \mathrm{FF}}{\mathrm{PD} \times \mathrm{A}} \times 100\%, \tag{3}$$

where $\mathrm{P_{max}}$ is the maximum power of the battery, $\mathrm{P_{source}}$ is the power of the radioisotope, $\mathrm{I_{sc}}$, $\mathrm{V_{oc}}$, and FF are the short-circuit current, open circuit voltage, and fill factor of the battery, respectively, and PD, A stand for power density and source area as in Eq. (1). In specific case of β-voltaics, many authors use the Shockley–Queisser approximated model to calculate the maximum achievable PCE, or more specifically the semiconductor conversion efficiency (SCE), related to internal processes in the semiconductor. The SCE can be calculated based on the bandgap value $\mathrm{E_g}$, electron backscatter coefficient f, and electron–hole collection efficiency Q:[26,27]

$$\mathrm{SCE} = \frac{\mathrm{V_{OC}FF}}{\varepsilon}, \tag{4}$$

$$\varepsilon = 2.8\mathrm{E_g} + 0.5\mathrm{eV}, \tag{5}$$

$$\mathrm{V_{OC}} = \frac{\mathrm{kT}}{\mathrm{q}} \ln\left(\frac{\mathrm{J_{SC}}}{\mathrm{J_0}} + 1\right), \tag{6}$$

$$\mathrm{J_{SC}} = \mathrm{q}(1 - \mathrm{f})\mathrm{Q}\left(\frac{\mathrm{P_{source}}}{\varepsilon}\right), \tag{7}$$

$$\mathrm{J_0} = 1.5 \times 10^5 \exp\left(-\frac{\mathrm{E_g}}{\mathrm{kT}}\right), \tag{8}$$

$$\mathrm{FF} = \left[\frac{\mathrm{V_{OC}}}{\mathrm{kT}} - \ln\left(\frac{\mathrm{V_{OC}}}{\mathrm{kT}} + 0.72\right)\right] \times \left[\left(\frac{\mathrm{V_{OC}}}{\mathrm{kT}}\right) + 1\right], \tag{9}$$

where ε is ionization energy of one electron–hole pair, T is temperature, q is the electron charge, and $\mathrm{J_0}$ is the saturation current.

Striking parallels may be observed between the fields of high energy particle detectors and nuclear batteries. In both cases, the ability to convert high energy particles to detectable light or detectable current is critical for optimal performance. However, unlike the fields of detectors, nuclear batteries require the following considerations: first, there is a specific need for compactness of the battery as to address the requirement of miniaturized electronic devices; second, the application of nuclear batteries in remote, inaccessible places creates the demand on a very long lifetime of the device, as they are designed for being maintenance-free; and lastly, the nuclear batteries are not oriented for information acquisition but purely energy capture, where the utilization of combined radiation types or combined RVB/RPVB effects could also be possible.

III. CURRENT STATUS OF NUCLEAR BATTERIES

The current state of nuclear batteries, particularly focusing on RTGs and RVBs, reflects significant advancements in technology and application. RTGs have proven their reliability in powering space missions and medical devices, with ongoing improvements aimed at enhancing efficiency and longevity. In parallel, RVBs, though once considered less efficient compared to conventional batteries, are gaining renewed interest due to emerging applications in advanced electronics. Recent innovations in materials and design, including the use of wide bandgap semiconductors and nanocomposites, are driving substantial performance improvements in RVBs. These developments underline the critical role of nuclear batteries in providing long-lasting power solutions for specialized, extreme environments.

In comparison with chemical batteries, the RVBs and RPVBs are characterized by much larger specific energy (i.e., the amount of energy per unit mass), which comes with a cost of significantly lower specific power.[28] Such characteristics highlight their advantages for long-lasting and miniaturized power sources. Also, due to the fact that RVBs and RPVBs are all-solid devices, they are much less affected by extremely high or extremely low pressure and temperature conditions. Additionally, while the chemical batteries can easily degrade in the presence of moisture,[29] the nuclear batteries are much more moisture-resistant. Thus, at the moment, the nuclear battery solutions offer benefits mainly in remote, long-life operating devices in harsh environments, rather than in everyday use electronics; however with further improvement of power density, their contribution in the power sources market is expected to gradually increase.

A. Thermal conversion with thermoelectric generators

RTGs have made significant strides in powering space exploration missions and medical devices. Initially invented in 1954 by scientists Kenneth C. Jordan and John Birden, RTGs were designed to convert the heat produced by radioactive decay directly into electricity using thermocouples.[30] The first RTG, SNAP 3B, was launched in 1961, utilizing ^{238}Pu to power the Navy Transit 4A spacecraft.[31] Since then, RTGs have also been used on the Moon for experiments during the Apollo missions and in remote terrestrial locations by the U.S. Navy and Soviet Union, demonstrating their reliability and longevity in extreme environments.[31]

In addition to space applications, RTGs have been adapted for medical use, notably in powering pacemakers with plutonium cells. Although the program was eventually discontinued due to safety concerns, it highlighted the potential of nuclear batteries in medical devices requiring long-lasting power sources.[32] Recent advancements in RTG technology include the exploration of subcritical reactions to enhance energy output, which could reduce the amount of ^{238}Pu needed for missions.[33] This approach, proposed to NASA and studied at the Idaho National Laboratory, demonstrates the ongoing innovation in RTG design to increase efficiency and extend the lifespan of these power sources.[33] Furthermore, using the dual functionality of the rear mirror for band-edge spectral filtering, a thermo-PV efficiency of 29.1% at 1207 °C can be achieved for such an RTG design.[34] All developments underscore the critical role of RTGs in both space exploration and specialized medical applications, driving continued research and refinement of this technology.

B. Non-thermal conversion with semiconductor detectors and scintillators

The first RVB was demonstrated in 1954 by Paul Rappaport.[35] For decades, scientists and engineers have worked to improve the battery design; however, it remained costly and inefficient as compared to rapidly progressing lithium-ion batteries, which became a standard solution for powering modern electronic devices. However, with the technological and civic progress of the 21st century, there are emerging new fields that could strongly benefit from radiovoltaics, such as space exploration, robotics, and bionics. This again drives the interest of researchers toward novel designs and material solutions that could be used to increase the performance of RVBs. Notably, in the past few years, direct detection of radiovoltaics has seen some noteworthy progress with several companies already involved in the development and production of RVBs (Fig. 2). One of the most matured suppliers of market-ready β-voltaic solutions is CityLabs, USA, which offers ^{3}H-based batteries with output power from nano to microwatts and lifetimes in between 10 and 20 years. The size of the 100-μW battery is approximately $100 \times 45 \times 8\,\text{mm}^3$, and it weighs 7.5 g. In their portfolio, CityLabs mentions collaboration with the U.S. Department of Defense, Department of Health and Human Services, and NASA, reflecting the strategic demand for long-lasting power sources in the fields of health, defense, and space exploration. Specific applications in the health sector include providing power sources for leadless cardiac pacemakers and other implants. In defense and space exploration, there is a growing demand for stable and durable power sources that can withstand harsh conditions, such as large amplitudes of temperature and cosmic radiation. As such, β-voltaic batteries are tested for use in small satellites or autonomic probes to be deployed on the Moon for *in situ* analyses. Another US-based company, Widetronix, offers two types of β-voltaic power sources, Firefli-T and Firefli-N, that utilize ^{3}H and ^{63}Ni radioisotopes as β-emitters, respectively. Firefli-T has the maximum initial output power of 1 μW, while the Firefli-N is lower power, up to 500 nW. Widetronix integrates their β-voltaic power sources with low-power consumption electronics, targeting duty cycled applications, which rely on running short operations on a periodic basis for long periods of time. This approach is particularly suitable for designing long-life remote sensors, capable of transmitting lesser amounts of data, that can be used in monitoring medical implants, industrial sites (i.e., oil or chemical industries), or defense equipment. Recently, there has been an announcement from China-based startup, Beijing Betavolt, that plans to revolutionize the market of β-voltaic battery with their BV100 power source capable of operating for 50 years continuously. The $15 \times 15 \times 5\,\text{mm}^3$ sized battery delivers 100-μw power, and it is based on ^{63}Ni radioisotope and diamond semiconductor modules.

1. Direct conversion with silicon carbides and other group IV semiconductors

Table II lists chosen experimental demonstrations of direct conversion radiovoltaic devices with various semiconductor materials. The advantage of using SiC and other WBGSs for radiovoltaic purpose was predicted in mid-1970s[26,36] when the relation between electronic bandgap and achievable PCE was first uncovered.

The first demonstration of SiC-based β-voltaic devices dates to 2006 work by researchers from Cornell university[37] and parallel report from Qynergy Corporation and University of Missouri.[20] Both groups reported a significant increase in PCE of SiC batteries (6%,[37] 4.5%[20]) as compared to previously demonstrated Si β-voltaic devices. SiC comes in a variety of forms, among which the high bandgap ones, such as 4H-SiC, are preferable. Noteworthy progress achieved in the manufacturing technologies, quality, and cost-effectiveness of SiC since the beginning of 21st century led to further improvement in SiC-based radiovoltaic technology, as new designs have been proposed and better performances achieved. In 2016, Thomas *et al.*[22] demonstrated 12% efficiency 4H-SiC β-voltaic battery using ^{3}H as β-electron source. In this work, a thin 200-nm 4H-SiC PN junction was used to optimize the capture of low energy β-electrons. Further improvements were

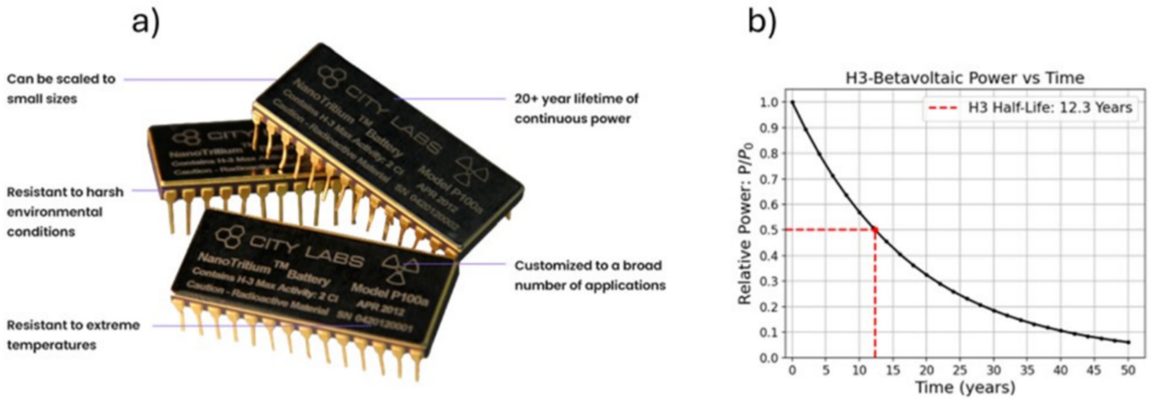

FIG. 2. Example of commercially available β-voltaic product. (a) CityLabs' NanoTritium battery. Reproduced with permission from CityLabs, Inc. (https://citylabs.net/wp-content/uploads/2022/12/technology-chip-graphic.png.webp).[133] (b) The performance of ^{3}H β-voltaic battery vs time. Reproduced with permission from CityLabs, Inc. (https://citylabs.net/wp-content/uploads/2023/02/download.png.webp).[134]

TABLE II. Chosen experimental demonstrations of RVBs with the information on semiconductor material, its bandgap value, radiation source and type, and the reported PCE, either directly measured (M) or estimated on theoretical grounds (E).

Semiconductor material	Bandgap (eV)	Radiation source	Radiation type	Measured/estimated PCE (%)	Reference
4H-SiC	3.26	^{3}H	β	$12^{M}/23^{E}$	22
4H-SiC	3.26	He-ion accelerator	α	0.88^{M}	42
GaN	3.4	Electron gun	β	4.5^{M}	52
Al-doped GaN	⋯	He-ion accelerator	α	4.51^{M}	54
Diamond	5.5	Electron gun	β	28^{M}	46
Diamond	5.5	^{238}Pu	α	3.6^{M}	23
TiO_2 nanotube arrays	3.2	^{63}Ni	β	26.55^{M}	58
$(FA_{0.85}MA_{0.15})_{0.9}Cs_{0.1}PbI_{2.55}Br_{0.45}$	1.6	Electron gun	β	$3.56^{M}/21^{E}$	92
$MAPbBr_3$	2.31	Electron gun	β	5.35^{M}	94
CdTe	1.51	^{3}H	β	0.0097^{M}	110

proposed with optimizing the junction depth or doping level,[38] composition of the junction,[24] or utilizing β-electrons with higher energy.[39] Recently, He *et al.*[12] proposed a three-dimensional (3D) $P^{+}PNN^{+}$ SiC-based junction design, for increasing the output power of the device to satisfy the power needs of micro-electro-mechanical-systems (MEMS). In this scheme, an array of micro-grooves is etched into the semiconductor junction and filled with ^{63}Ni radioisotope. Fabrication of 3D β-voltaic designs has been demonstrated before with Si-based junctions; however, it poses a significant technological challenge.[40] Alternatively, to β-voltaics, the use of SiC for α-voltaic devices has been investigated. The first reports date back to 1999;[41] however, the achieved efficiency was exceptionally low (PCE $< 0.1\%$) and the devices showed rapid degradation in time. Later on, the improved lifetime in the SiC Schottky barrier diode based α-voltaic cells was reported with the use of lower activity sources,[3] however, with no improvement of the PCE. Gao *et al.*[42] suggested an optimized design to increase efficiency without the necessity of using a source with higher activity. Up to date, the radiation induced degradation remains the largest obstacle in the development of SiC-based α-voltaics. One potential solution for the future is in exploring the combined junction architectures with Si and SiC.[43] Because of the high radiation damage caused by α particles to semiconductors, some researchers try to use diamond-based Schottky barrier diodes[23,44] for α-voltaic energy conversion, as diamond resistance to ionizing radiation is outstanding.[45] Diamond also shows remarkably high efficiency as β-voltaic converter, close to the theoretical Shockley–Queisser limit,[46] and it is considered a promising material candidate for direct scheme γ-voltaic,[47] which is difficult to achieve with other semiconducting materials. Despite its highly advantageous material characteristics, the cost of diamond films is a strong limitation to its use in larger scale applications.

2. Direct conversion with III-V semiconductors

Among III-V semiconductors, there are some with sufficiently wide bandgap to become suitable candidates for radiovoltaic purpose, including GaP (bandgap of 2.26 eV)[26] and GaN[48,49] (bandgap of 3.44 eV). Because of large bandgap value, particularly good electronic properties, and very advanced technology of manufacturing, GaN became the main alternative to SiC for the use in direct β-voltaic devices. The first demonstration of GaN-based β-voltaic device was made by Lu *et al.*[48] in 2011, who reported the PCE 0.32% and V_{oc} 0.1 V with Schottky barrier diode architecture. The achieved performance was limited due to thin effective energy deposition layer. An improved efficiency of 2.7% V_{oc} of 1.65 V was claimed by Cheng *et al.*[49] who used GaN PIN homojunction. Later in 2013, it was shown that with then available GaN growing techniques, the PCE of 2.25% would be achievable with GaN-based Schottky β-voltaic battery.[50] In the next years, several authors studied optimized designs for the GaN based junctions to increase the achievable PCE.[24,51–53] Up to date, the highest experimentally obtained value of PCE for GaN-based β-voltaics is 4.5%.[52] As for the α-voltaic cells, the first such device utilizing GaN-based junction has been only recently demonstrated by Gao *et al.*,[54] who used GaN with isoelectronic aluminum doping. The authors reported high efficiency of 4.51%, which is comparable with state-of-the-art GaN-based β-voltaics. Also, the lifetime of the device was estimated as 15 000 h under 0.05 mCicm^{-2} α-source. The authors concluded that further increase in PCE is needed for reducing the activity of the source and thus increasing the battery lifetime.

3. Direct conversion with nanocomposites and 3D junction architectures

In sandwich-type one-dimensional (1D) β-voltaic architectures, the β-electron collection efficiency is significantly limited due to self-shielding of the source as well as the junction region area per unit volume. To address this challenge, several groups investigated the β-voltaic cells with 3D architectures that can reach higher PCE than their 1D counterparts. In one of the first demonstrations, Sun *et al.* reported ten times PCE enhancement using porous Si PN junction as compared to reference planar junction.[55] Later on, Zhang *et al.*[56] proposed to use TiO_2 nanotube (TNT) arrays, nanostructured material with big PV capabilities[57] and wide bandgap 3.0–3.2 eV. The authors demonstrated a β-voltaic device based on metal/semiconductor/metal architecture, specifically ^{63}Ni/TNT/Ti, that shows β-voltaic effect under built-in voltage due to contact potential difference between Ni and Ti. The device showed effective PCE (using effective source activity) as high as 7.3%, which is significantly higher than conventional SiC or GaN based planar detectors. In continuation of this research, the same group reported β-voltaic enhancement with TNT/graphene oxide nanocomposite [Fig. 3(a)] and they claimed high value of PCE equal 26.55%.[58] One more study reported free-standing ZnO nanorod arrays (bandgap of 3.37 eV) that were combined with metallic single-wall-carbon-nanotubes (m-SWCNTs) to form a 3D Schottky junction.[59] The use of m-SWCNTs aims to suppressing carrier recombination and increasing the β-electron absorption at the same time. The operation of the device was demonstrated for both PV and β-voltaic effect with the β-voltaic PCE equal to 3.58%. Recently, another strategy has been reported for enhanced β-voltaic performance based on interfacial electrochemical engineering of the WBGS nanostructure [Fig. 3(b)].[60,61] Hwang *et al.*[61] used ruthenium-sensitized TiO_2 as anode, ^{14}C quantum dots (QDs) as the source/cathode, and polyiodide solution I^{3-}/I^{-} as liquid electrolyte that facilitates the β-generated charge transport [Fig. 3(c)]. Wang *et al.*[60] previously mentioned SWCNT/TNT and composites[59] were also filled with polyiodide solution and reported β-voltaic enhancement due to better charge transport and separation. The achieved total efficiency was 8.74%, one of the highest reported for β-voltaic cells using WBGSs.

4. Indirect conversion mediated by conventional scintillators

The indirect radiovoltaic conversion devices or RPVBs were first introduced in the early 21st century as a solution to prominent level of degradation caused by energetic α- and β- particles to semiconducting heterostructures in direct radiovoltaic devices. Commercial scintillating materials, such as lanthanide crystals, possess greater radiation hardness than most of the semiconductor materials used in RVBs, and so they can provide longer battery life and better stability, even though the achievable power output might not be high. Table III lists the experimental demonstrations of indirect radiovoltaic conversion, with various choices of scintillator and PV material. Sychov *et al.* reported the optimized design of the RPVB with ^{238}Pu as α-radiation source.[62] The authors tested several scintillating materials, including yttrium aluminum garnet, ZnS, oxides, oxysulfides, SiAlON:Eu, and tiogallates. They chose (Zn,Mg)F_2:Mn as the most stable one under ^{238}Pu exposure and reported 19% of radioluminescence loss after 411 h of continuous irradiation. Another comparative study has been conducted by Hong *et al.*[63] regarding the performance of RPVB with ZnS:Cu or Y_2O_2S:Eu as scintillator, ^{147}Pm as β-source, and GaAs PV cell. In that work, the ZnS:Cu yields better PCE; however, the achieved value is low as it equals 0.04%. ZnS:Cu for RPVBs has been investigated in other works that concerned design issues of the scintillating layer and its integration with the rest of the device.[64–66] Xu *et al.*[64] discussed the V-grove structure on the scintillator surface that produces 2.46 times enhancement of the maximum output power. Jiang *et al.*[65] reported an improved sandwich design of the RPVB that allows for better light coupling between scintillating film and PV cell [Fig. 3(d)]. This

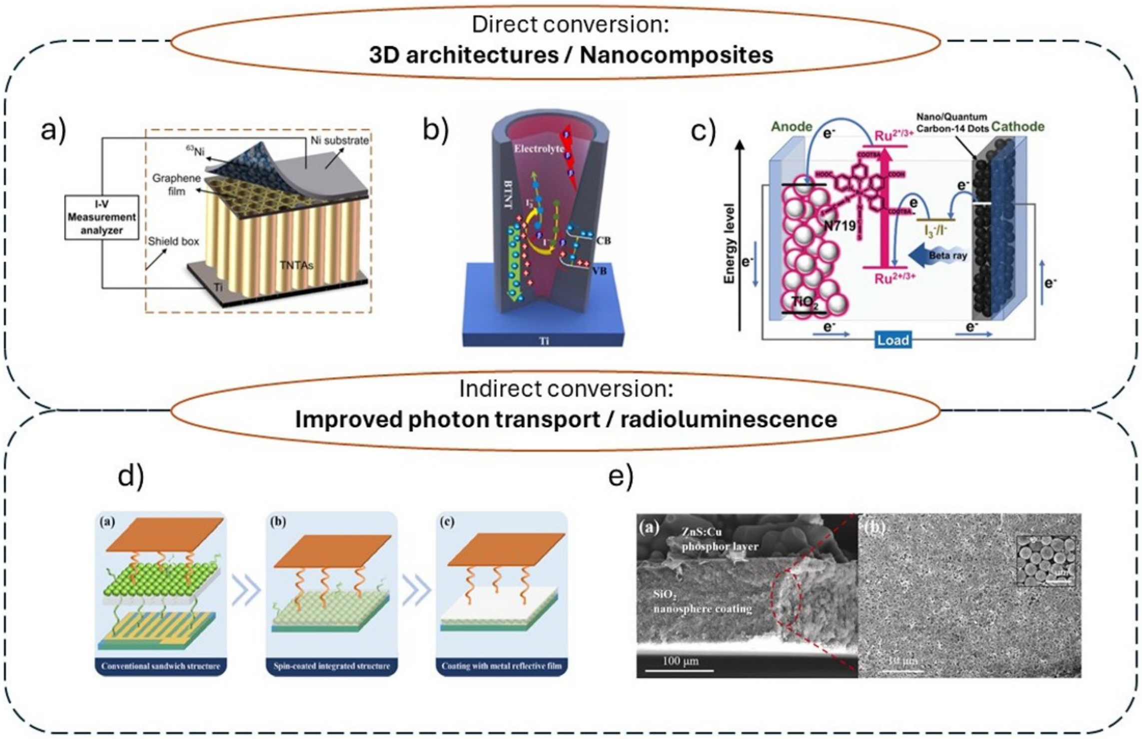

FIG. 3. Modern research trends in direct and indirect radiovoltaic conversion scheme. (a) Graphene oxide deposited on TiO_2 nanotubes for enhanced β-voltaic response. Reproduced with permission from ACS Appl. Mater. Interfaces **8**, 24638–24644 (2016). Copyright 2016 ACS Publications.[58] (b) Electrochemical β-voltaic cell based on carbon and TiO_2 nanotubes. Reproduced with permission from Compos. B Eng. **239**, 109952 (2022). Copyright 2022 Elsevier.[60] (c) C-14 powered β-voltaic cell based on dye-sensitized TiO_2. Reproduced with permission from Chem. Commun. **56**, 7070–7083 (2020). Copyright 2020 Royal Society of Chemistry.[61] (d) Optimizing the device architecture to improve the photon transport from scintillator to PV. Reproduced with permission from J. Sci.-Adv. Mater. Dev. **8**(3), 100611 (2023). Copyright 2023 Elsevier.[65] (e) SiO_2 nanospheres for increasing the efficiency of ZnS:Cu as scintillator in nuclear batteries. Reproduced with permission from J. Lumin. **255**, 119600 (2023). Copyright 2023 Elsevier.[66]

TABLE III. Chosen experimental demonstrations of RPVBs with the information on scintillator and PV material, radiation source and type, and the reported PCE, either directly measured (M) or estimated on theoretical grounds (E).

Scintillator material	PV material	Source	Radiation type	Measured/theoretical PCE (%)	Reference
ZnS:Cu	GaAs	^{147}Pm	β	0.04^{M}	63
ZnS:Cu	AlGaInP	^{63}Ni	β	0.92^{E}	65
LYSO	GaAs	^{60}Co	γ	$0.0235^{M}/0.52^{E}$	25
ZnS:Ag	$Cs_{0.15}FA_{0.85}Pb(I_{0.95}Br_{0.05})_3$	He-ion accelerator	α	0.886^{M}	93
TbMel	$Cs_{0.05}MA_{0.1}FA_{0.85}PbI_3$	^{243}Am	α	0.889^{M}	98
$Cs_3Cu_2I_5$:Mn	GaAs	x-ray tube	x-ray	⋯	95
$Cs_3Cu_2I_5$:Tl	Si	x-ray tube	x-ray	⋯	97

enhancement is based on index matching and reflection from additional metallic film that can increase output power of the device by 52.6%. This study expected the improved device architecture to reach maximum PCE of 0.92%. Also, 51.59% enhancement of output power is reported with the use of SiO_2 nanosphere coating combined with ZnS:Cu scintillator layer [Fig. 3(e)].[66]

Another issue regarding the α- and β- radiation interacting with the scintillator is that the latter can play a dual role:[67] it converts the particle energy to visible light, while it also works to decrease the kinetic energy of the incoming particles, making them easier to absorb in the semiconductor heterostructures. Xue *et al.*[67] explored these benefits as they reported PCE enhancement in hybrid direct/indirect α-voltaic device that uses SiC-based Schottky diode coupled to ZnS:Ag or LYSO scintillator film. It is noted that the choice of the scintillator should be matched with the PV detector characteristics, as the match level significantly affects the device performance.[63,67]

Apart of the lifetime issues, the indirect conversion scheme creates the opportunity to exploit radioisotopes with significant γ radiation. As mentioned in Sec. III B, direct scheme γ-voltaics is challenging due to exceedingly long absorption lengths of γ photons in most semiconductors. Lanthanide scintillators can be used to efficiently convert γ radiation to visible light. Zhang *et al.*[68] studied the performance enhancement of the GaAs γ-voltaic by addition of the 2-mm thick Y_2SiO_5 crystal and reported over four times increase in both output power and PCE, with the total PCE equal to 2.31%. Guo *et al.*[25] demonstrated a multilevel γ-voltaic cell based on a number of stacked GaAs PV cells and layers of LYSO scintillator. The authors estimated the contribution of both direct radiovoltaic and indirect radio-PV effect on the overall power conversion and concluded that both effects play significant role.

C. Current application limitations

Non-thermal conversion nuclear batteries are mostly aimed for the applications in small size, remote, low power consumption electronics, which are difficult to sustain for longer operation time with conventional power sources. The state-of-the-art RVBs and RPVBs can provide PD from tens of nW/cm^2 to tens of μW/cm^2, depending on the configuration used. However, larger power densities usually come with a cost of a shorter lifetime as they require the use of higher activity sources or more energetic radioisotopes. Output power can be scaled with the junction and radioisotope effective surface, but keeping the size of battery up to few mm^2 can be essential for many low power electronic devices. Thus, it is the trade-off between battery size, output power, and lifetime that decides about profits delivered by radiovoltaic solutions in specific fields. For instance, in the application of MEMS, the battery size at the order of mm^2 is desired,[69] and the required power output is in the range of 1–100 μW.[70]

With the achievable power densities of RVBs and RPVBs, meeting such a goal is still challenging. New junction architectures, new energy conversion materials, or precise bandgap engineering are then required to successfully address the power needs of modern microelectronics with long (few year) lifetime requirement. Some of the current materials science research trends for increasing the performance of nuclear batteries will be overviewed and discussed in Secs. IV and V, which includes MPHs and MCs for direct and indirect conversion schemes.

IV. PROSPECTS OF METAL PEROVSKITE HALIDES

Perovskite materials have been in the spotlight since the past decade due to their simple and cost-effective synthesis methods and outstanding optical properties across the visible wavelength range.[71,72] The general formula for halide perovskites is ABX_3, where A and B are monovalent and divalent cations, respectively, and X is a halide (Cl, Br, or I). Lead-containing perovskites have become popular in optoelectronic devices like solar cells, light emitting diodes (LEDs), photodetectors, and scintillators.[73–75] However, these perovskite materials are susceptible to degradation from moisture due to the volatile organic component ($CH_3NH_3^+$) and its very unstable crystal structure. The structure consists of the A cation occupying the body center of a cube with corner-sharing $[BX_6]$ octahedra forming a 3D network. Site A accommodates larger cations while the B-site hosts smaller transition metal cations, with the X anion residing at the center of each octahedron. In an ideal perovskite structure, the B–X distance is equal to $a\sqrt{2}$ and the A–X distance is $a\sqrt{2}/2$, where a is the lattice constant of the cube. The radii of the constituent atoms fulfill the equation: $R_A + R_X = \sqrt{2}(R_B + R_X)$. Goldschmidt found that the perovskite structure is retained even when the ABX_3 compounds do not exactly obey this relation and defined a tolerance factor t given by

$$t = \frac{R_A + R_X}{\sqrt{2}(R_B + R_X)}. \tag{10}$$

For an ideal perovskite structure, it is unity. Distortions in the structure lead to reduction in t till $t \geq 0.75$. Although the t value greater than 0.8 is considered to the empirical stability range for ionic oxides, higher covalence in MPHs and the non-spherical shape of their A-cations (methylammonium and formamidinium) led to the observation that stable perovskites can only be expected for $t > 0.9$. The highest symmetric crystal structure of perovskites belongs to the $Pm\overline{3m}$ cubic space group. Most perovskites are hettotypes owing to lattice distortions in the form of tilted octahedra, cationic or anionic vacancies, anti-site ions, and other lattice defects. To improve the stability of hybrid perovskites, researchers have developed several methods, including the use of anti-solvents during film formation and various encapsulation techniques.[76] Recently, two-dimensional (2D) perovskites have garnered significant interest for their enhanced stability and moisture resistance compared to three-dimensional (3D) perovskites.[77] Represented by the formula $R_2(CH_3NH_3)_{n-1}B_nX_{3n+1}$, where n represents the number of inorganic layers, R is an organic cation (such as phenyl-ethyl ammonium), B is a metal cation, and X is a halide, these 2D perovskites benefit from the hydrophobic R group.[78,79] This group occupies the surface of the crystals, preventing water penetration. Despite their promise, further research is necessary to optimize these materials for practical, real-world applications.

As the B-site cation in the ABX_3 structure is usually a heavy transition metal, perovskites form bandgaps in the visible to near infrared (IR) range, high absorption coefficient (10^4–$10^5\,cm^{-1}$), high photoluminescence quantum yield (PLQY), and exceptionally long carrier diffusion lengths (several micrometers) and lifetimes (in the microsecond range), causing them to be of interest in PVs, light-emitting diodes, phototransistors, and scintillators. $MAPbX_3$ perovskites show significant hydrogen bonding between the organic moieties and the halides, which give rise to exceptional optoelectronic properties.[80,81] The bandgap of MPHs can be tuned by changing the composition ratio of halides and the size of the MPHs nanocrystals (NCs) (due to quantum effects), which affect their absorption and emission peak wavelengths. Especially, $CsPbX_3$ NCs have been found to emit bright red-green light with high PLQY of 50%–90% without the advantages of core–shell passivation and narrow emission line widths of 12–42 nm.[82] The PL full-width-at-half-maxima (FWHM) of perovskite NCs is narrower than most other types of QDs. Such high PLQYs occur due to the defect-tolerant nature of MPHs NCs. Here, the term "defect tolerance" means, although the optical and electronic properties of perovskites often appear to be void of traps, structural and other characterizations do reveal varied structural defects. Such behavior suggests preservation of a clean bandgap upon formation of common defects like vacancies, as their defect energy states lie entirely within the valence or conduction band, but not within the bandgap itself.

Despite its fascinating features, lead halide perovskites are still a long way off from being used in commercial devices. Through improved material engineering, the performance of optoelectronics based on perovskite has significantly improved in just a year, spurring future studies in this area to reach higher efficiency. However, it is crucial to remember that these devices' operational lifetimes are still quite short, and a complete knowledge of the processes leading to degradation is still a long way off. Recently, perovskites also have shown their potential in detecting high-energy radiation such as x-rays and γ-rays.[8,83–87] Their high atomic number components and good charge transport properties allow for efficient absorption and conversion of high-energy photons into electrical signals. However, the understanding of how high energy radiation affects the stability and morphology of the perovskite lattice in the first place, which is crucial for unlocking their full potential in device applications. Song *et al.*[88] proposed that imaging of halide perovskites using transmission electron microscopy (TEM) is challenging because of the extreme sensitivity of their structures to the electron beam. Therefore, covering both all-inorganic and organic–inorganic hybrid MPHs, with an emphasis on the specific imaging conditions that have proven to be effective in avoiding electron beam-induced structural damage. Hence, Bose *et al.* have systemically tracked the behavior of the perovskite lattice when exposed to a beam of electrons for atomic scale imaging purpose at ambient temperatures and remarkably captured the point of transition of the perovskite NCs from its most stable cubic phase to the less stable orthorhombic phase, which has not been reported till date.[89] The proposal of the energetics of the electron-irradiated perovskite lattice that govern the phase transformation from the cubic to the orthorhombic phase using Density Functional Theory is also reported for the first time. Nowadays, Kirmani *et al.*[90] investigated radiation damage and healing mechanisms in perovskite halides using energy-tuned dual irradiation dosing. They found direct proof of radiation-induced efficiency recovery in perovskite solar cells. The design of dual dose proton irradiation experiments allows us to uniquely tune radiation–matter interactions in the devices. This investigation reinforces the growing understanding that radiation matter interactions in perovskite solar cells are quite different from conventional space PV and present dual dose irradiation experiments as a unique platform to tune and heal defect densities within perovskite thin films. However, Zaffalon *et al.*[91] demonstrated the exceptional radiation hardness of $CsPbBr_3$ NCs that retain their initial RL efficiency after exposure to as much as 1 MGy of delivered γ-ray dose, corresponding to the annual dose accumulated by the inner walls of a nuclear reactor chamber and by the inner magnetic coil of the Large Hadron Collider at CERN. This provides valuable guidelines for highly efficient radiation hard devices to be produced via chemical methods, which strengthens the potential of lead perovskite halides nanostructures in real-world radiation detection.

Halide perovskite emerges as a promising candidate for next generation radiovoltaics due to its long carrier diffusion length, high defect tolerance, strong β-particle interaction, and adjustable bandgap. With their properties, perovskites hold potential to be used as junction materials in RVBs and in scintillating energy converters or the PV components of the RPVBs. Despite that, research on perovskite-radiovoltaic devices remains scarce. Song *et al.* demonstrated a prototype perovskite-β-voltaic cell with a PCE of 3.56%, tested under electron radiation mimicking a 10 keV and 253 mCi source using an electron gun.[92] Geant4 simulation results suggest an excellent PCE of 21.0% for ^{63}Ni perovskite-β-voltaic devices as shown in Fig. 4(a). Gao *et al.* reported a radio-PV cell as presented in Fig. 4(b) based on a formamidinium–cesium perovskite converter, which displayed a broad light wavelength response (300–800 nm), high open-circuit voltage, and PCE of 0.886% at low-light intensity, outperforming the Si reference cell by 6.6 times.[93] In another study, high-performance perovskite β-voltaic cells using thick, high-quality, wide-bandgap $MAPbBr_3$ polycrystalline achieved a PCE of 5.35% under 15-keV electron radiation equivalent to a 253-mCi source as displayed in Fig. 4(c).[94] Low-dimensional materials and quantum dots (QDs) have also been employed as shown in Figs. 4(d)–4(f) to achieve high light yield scintillators and to tailor luminescence and stability through Mn doping[95] or optimizing the halide composition.[96] We note that among many promising perovskite

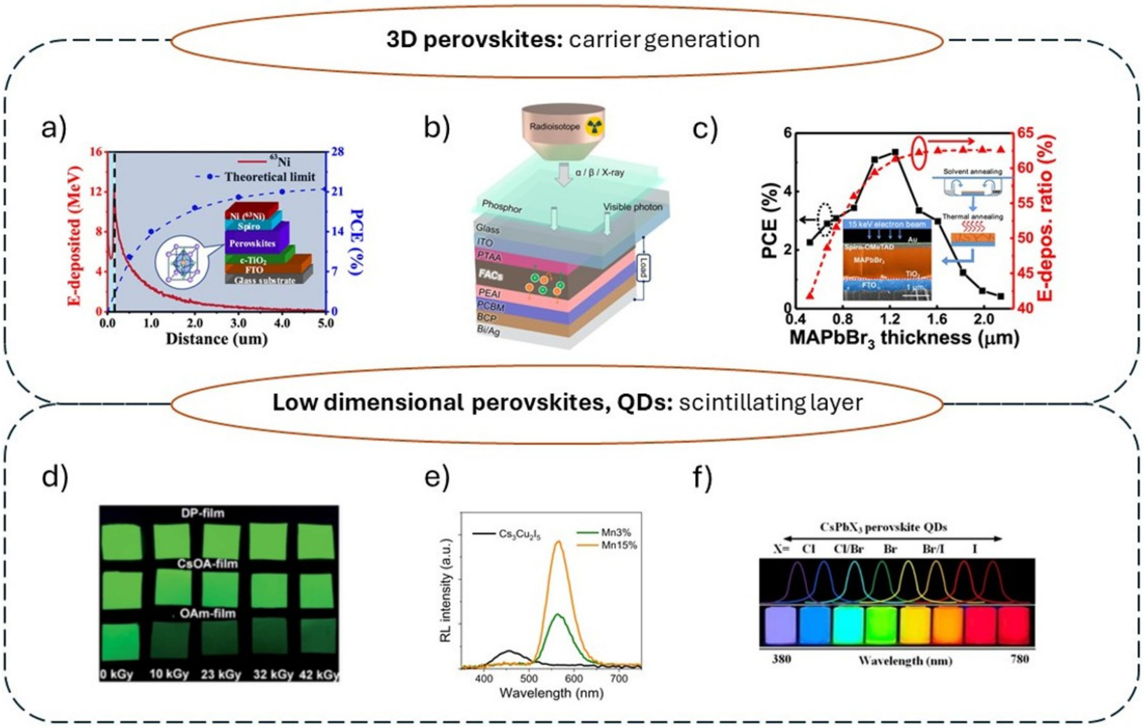

FIG. 4. Research on perovskite use for nuclear batteries. (a) Mixed-ion perovskites. Reproduced with permission from ACS Appl. Mater. Interfaces **11**, 32969–33297 (2019). Copyright 2019 ACS Publications.[92] (b) Formamidinium–cesium perovskites. Reproduced with permission from Energy Environ. Mater. **7**, e12513 (2022). Copyright 2022 Wiley Onlice Library.[93] (c) High-crystallinity methyl-ammonium perovskites for charge separation layer. Reproduced with permission from ACS Omega **6**, 20015–20025 (2021). Copyright 2021 ACS Publications.[94] (d) Radiation stability for CsPbBr$_3$ QDs with different shelling. Reproduced with permission from J. Mater. Chem. A **9**, 8772–8781 (2021). Copyright 2021 Royal Society of Chemistry.[99] (e) Mn doping of cesium copper halides for achieving high light yield scintillator. Reproduced with permission from Nat. Commun. **12**, 3879 (2021). Copyright 2021 Springer Nature.[95] (f) Optimizing CsPbX$_3$ halide composition for tailoring the luminescence and stability. Reproduced with permission from ACS Appl. Mater. Interfaces **11** (15), 14191–14199 (2019). Copyright 2019 ACS Publications.[96]

materials for nuclear battery applications, the cesium copper halides hold particularly great promise, due to extraordinary radioluminescence light yield, low self-absorption and low toxicity, which is reflected in growing interest in these materials for nuclear battery applications.[95,97] Gao *et al.* demonstrated 98 000 ph/MeV radioluminescence light yield from Tl-doped $Cs_3Cu_2I_5$, and RPVB based on this material, that provided high power density 898 nW/cm^2.[97]

Recently, Li *et al.* demonstrated an innovative design of RPVB, based on scintillating coalescent energy transducer and perovskite PV cell.[98] Mixed cation $Cs_{0.05}MA_{0.1}FA_{0.85}PbI_3$ perovskite has been selected due to its good optoelectronic properties, high stability, and large overlap of its absorption spectrum with the emission of coalescent energy transducer. The concept of coalescent energy transducer is based on coupling of the α-particle source ^{24}Am with scintillating material on the molecular level. This is favorable for improving the PCE of the device due to diminished self-absorption of emitted α particles and also better energy deposition in the scintillator. The PCE of 0.889% is reported, which is the highest measured value among all the experimental demonstrations of RPVB devices up to date.

It is worth noting that with their diverse chemical tuning options and possible low self-absorption formulas, perovskite scintillators are also suitable to be combined with radioisotope on a deep level. One of the critical challenges in the development of scintillator materials is self-absorption, where the emitted light is reabsorbed by the material itself, reducing overall efficiency. By developing low self-absorption perovskites, it becomes possible to fabricate thicker scintillator layers that can capture more high-energy radiation and generate increased luminescence signal that can reach the detector, resulting in better energy conversion efficiency. Low self-absorption perovskites can be engineered by optimizing the composition as shown in Fig. 4(f) and structure to minimize the overlap between the emission and absorption spectra.[95] Techniques such as doping with specific elements as shown in Fig. 4(e) or creating quantum dot structures [see Fig. 4(d)] can enhance the emission properties while reducing reabsorption.[99] This improvement would allow for the design of more effective and efficient scintillators, capable of higher light yields and better performance in radiovoltaic applications. Integrating radioactive sources directly into perovskite films with optimized self-absorption could become another groundbreaking development in the field. The direct incorporation of radioactive sources can enhance the interaction between energetic particles and the perovskite material, reducing energy losses associated with the separation of the radiation source and the converter. Developing stable and safe methods for incorporating radioactive materials into perovskite films is crucial. This includes ensuring the uniform distribution of isotopes within the perovskite matrix and maintaining the structural integrity and performance of the perovskite material. An advanced synthesis techniques and material engineering will play a significant role in achieving this integration.

Advancements in low self-absorption perovskites and the incorporation of radioactive sources into perovskite films could significantly impact various fields. These technologies promise more efficient nuclear batteries and the improved power output required for targeting new applications such as MEMS. Improvements could be also made to space exploration application, where long-lasting, reliable power sources are essential, and to medical devices, where compact, high-efficiency power supplies can enhance the functionality and longevity of implants and sensors.

V. PROSPECTS OF METAL CHALCOGENIDES

MCs can be described as binary compounds composed of transition metals, alkaline earth, and basic metals as active A site accompanied by chalcogenide (O, Se, Te, and S) elements. Due to their fascinating electronic and optical properties, these materials could be beneficial toward their implementation in nuclear battery technology. The conception of chalcogenides as active components in nuclear batteries is quite intriguing in terms of direct applications for RTGs. The thermoelectric properties of RTGs have shown that a good power efficiency of such batteries is attainable in the current development. Owing to their excellent thermoelectric properties, MCs promote heat into electricity conversion rate by collecting thermal energy from radioactive decay process.[100–104] In line with the good thermoelectric properties, these materials possess excellent thermal stability in high-temperature application as converter of the collected thermal energy from atomic decay.[105] Thermoelectric materials performance is harnessing Seebeck effects, and this can be determined based on the following dimensionless merit:

$$ZT = \frac{S^2\sigma T}{\kappa} = \frac{S^2\sigma T}{(\kappa_L + \kappa_E)}, \tag{11}$$

where S is Seebeck coefficient, σ is the electrical conductivity, κ is the thermal conductivity consists of total lattice thermal conductivity (κ_L) and electronic thermal conductivity (κ_E), and T is the absolute temperature.[106] Seebeck coefficient could be enhanced significantly by manipulating temperature control with respect to the charge mobility variation. Due to different charge mobilities gradient across two distinct charge-relaxation regimes within a material, an electrical potential could be generated to modify the density of the states (DOSs). This in turn allows to mobilize the electron relaxation, which is crucial toward thermal energy conversion.[107] Telluride-based MCs are widely used in thermoelectric applications and can be used as active material of nuclear batteries. Assoud *et al.* reported $SrSc_2Te_4$ and $BaSc_2Te_4$ exhibit an identical flat band slopes around the Fermi level, yielding high Seebeck coefficient with the values of 415 and 270 μV/K for $SrSc_2Te_4$ and $BaSc_2Te_4$, respectively. In their study, $SrSc_2Te_4$ and $BaSc_2Te_4$ categorized as extrinsic semiconductors since both display narrow bandgap gaps of 0.1 and 0.2 eV, respectively. In addition, these MCs possess low electrical conductivity at room temperature 1.5 $m\Omega^{-1}\,cm^{-1}$ ($SrSc_2Te_4$) and 2.6 $m\Omega^{-1}cm^{-1}$ ($BaSc_2Te_4$). Telluride-based compounds also have been used as block thermocouples for rigid flexible thermoelectric generator of PP-PEDOT rolls. For example, Bi_2Te_3 provides a high thermoelectric output under ΔT of 7.9 K. Each of Bi_2Te_3 block contributes to the generation of 1 Ω resistance attributed to the connection resistance of legs and thermocouples. In addition, Bi_2Te_3 exhibits a quite impressive output power of thermoelectric modules including 607 pW/K/TC by 100 pieces CNT-Bi_2Te_3 and 404 pW/K/TC by 36 pieces PP-PEDOT-Bi_2Te_3.[108] Many studies have used bismuth tellurides as a component thermoelectric leg on a flexible circuit of RTG, such as reported in the study by Yuan *et al.*, who demonstrated ten layers of a prototype with ^{238}Pu radioisotope as a heat source that can generate the P_{max} of 114.38 μW at 0.408 V, short-circuit current of 0.551 mA, and open voltage of 0.815 V.[109] Apart from their advantages in thermoelectric applications, the MCs also hold potential to be used in non-thermal nuclear batteries such as semiconductor converters or scintillators. Lin *et al.* demonstrated the use of CdTe, a common material used in medical x-ray detectors, for RVBs.[110] Although the achieved experimental PCE is only 0.0097%, in future the CdTe material could attract more attention due to high radiation hardness and mature technology of manufacture. On the other hand, MCs could be potentially used as the fluorescent layer components of RPVBs. Xu *et al.* reported that the layer of ZnS–Cu with β source ^{147}Pm exhibits the good power output of radioluminescent nuclear battery reaching P_{max} almost 0.04 nW with the mass thickness ~13 mg/cm^2, while when source of ^{63}Ni, P_{max} is used, the power nearly reached about 0.03 nW. To enhance the radioluminescence emission intensity, CdSe/ZnS core–shell quantum dots in oil were used and thereby P_{max} can be increased from 1.01 to 15.48 times.[13,111]

Further development in the nuclear batteries technology by implementing MCs as active components holds a good promise, since the current interest is practically limited only to few chalcogens used in the thermoelectric materials or fluorescent layers. We, therefore, require exploiting our attention in using rational design to push the limit of thermoelectric properties and fluorescent materials to obtain high-power output of nuclear batteries. We also should aim for a clear route to achieve the good PCE of the chalcogenide perovskite films and high-performance perovskite β-voltaic as previously mentioned in the perovskite sections. For example, $BaZrS_3$ exhibits a good photoresponse activity with the bandgaps, electron, and hole mobility of ~1.85 eV, 16.8 cm^2/V s, and 2.6 cm^2/V s, respectively.[112] Due to such promising optoelectronic features, the maximum PCE ~30% with a device configuration $ZrS_2/BaZrS_3/SnS$ and $ZrS_2/Ba(Zr,Ti)S_3/SnS$ could be harvested.[113] In addition, $BaZrS_3$ and $BaHfS_3$ display remarkable photoluminescence (PL) after 16-h sulfurization. We infer such parameter could be technically beneficial in the improvement of radioluminescent nuclear batteries.[114] The 2D $^6LiInP_2Se_6$ semiconductor and CdSe/ZnS quantum dots[13] are state-of-the art MCs for direct radiation detections[8] and scintillation,[82] enhancing radiovoltaic devices, and non-thermal conversion batteries in radio PV systems, respectively. The $^6LiInP_2Se_6$ is particularly sensitive to α particles, making it an excellent candidate for use in α-voltaic semiconductors.[8] Additionally, CdS/CdSe/CdS colloidal quantum shell heterostructures[82] demonstrate exceptional performance, with light yields reaching up to 70 000 photons/MeV at room temperature, driven by their high multiexciton radiative efficiency.

VI. PHOTONIC AND PLASMONIC ENHANCEMENTS

Photonic- and plasmonic-based approaches have been proposed in recent years for improving the performance of scintillator systems,[115] based on phenomena such as Purcell enhancement[116] of spontaneous emission and improved light outcoupling. An overview of enhancement strategies is presented in Fig. 5. Nanostructured, layered, or nanocomposite media are emerging solutions for scintillation-

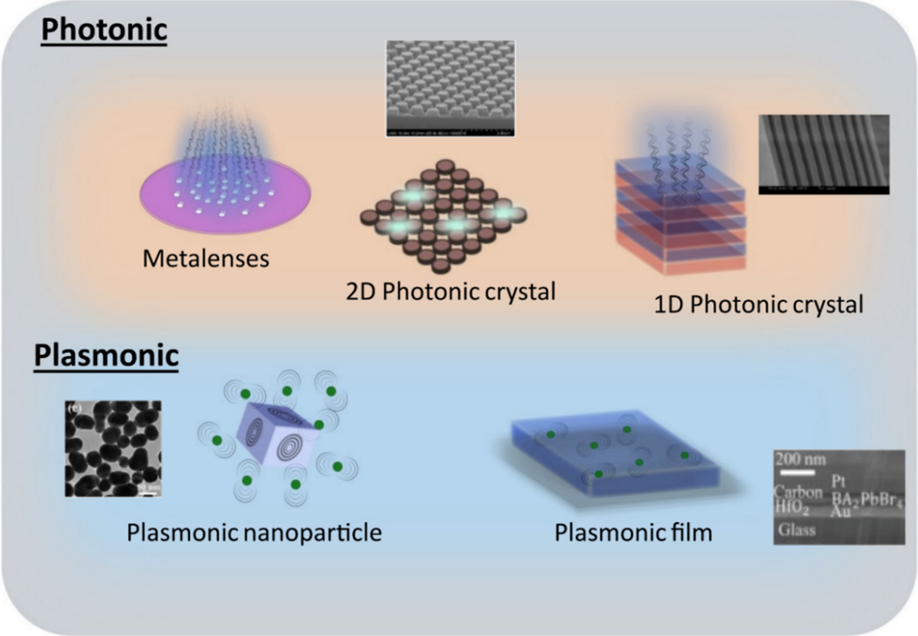

FIG. 5. Potential development for nuclear batteries: photonic and plasmonic scintillators. They include high-Q metalenses,[124] photonic crystals,[118,122,123,135] Bragg stacks,[125,126] plasmonic nanoparticles,[127,136] and plasmonic films.[83,115] 2D photonic crystal microscope image (middle top) was reproduced with permission from Crystals **8** (2), 78 (2018). Copyright 2018 MDPI.[118] 1D photonic crystals based on Si microscope image (right top) was reproduced with permission from Opt. Commun. **259**(1), 104–106 (2006). Copyright 2006 Elsevier.[135] Plasmonic nanoparticle microscope image (left bottom) was reproduced with permission from Nanoscale **7**(37), 15251–15257 (2015). Copyright 2015 Royal Society of Chemistry.[136] Plasmonic film microscope image (right bottom) reproduced with permission from Adv. Mater. **36**(25), 2309410 (2024). Copyright 2024 Wiley Online Library.[83]

based devices,[117] and their use in radiovoltaic may become another milestone in pursuit of higher power output batteries.

Historically, enhancing scintillator performance via nanophotonics has been limited to the application of nanophotonic coatings, typically designed as 2D structures with gratings.[118,119] These coatings address the challenge of photon emission blockage caused by total internal reflection, which often impedes the extraction of scintillation photons. By facilitating the transmission of photons that would otherwise be confined within single crystal scintillators, these photonic coatings significantly boost photon extraction efficiency. Recent advancements based on the Purcell effect have introduced innovative nanophotonic techniques to further refine scintillator performance. These techniques involve engineering scintillators into nanofilms or photonic crystals at the wavelength scale to not only boost photon extraction efficiency but more importantly to precisely enhance the intrinsic emission rate of the scintillator centers themselves. Noteworthy breakthroughs have demonstrated that integrating nanostructures including photonic crystals,[117,120] multilayer nanophotonic structures,[121] and nanoplasmonic system[83] can effectively tailor the decay time and light yield of scintillators through the Purcell effect. Such geometrical modifications complement other performance enhancement strategies, such as materials engineering, doping and co-doping, optical coupling, and circuit optimization. The implementation of nanophotonics thus offers the potential to push materials beyond the current limits of timing performance.

MPHs and MCs are especially well-suited for nanophotonics engineering-encompassing photonic and plasmonic Purcell and non-Purcell optimizations, for a number of reasons. These include due to their ability to be precisely tuned in terms of refractive index and bandgap, the convenience of deposition or processing methods, as well as the potentially low self-absorption of these materials to facilitate high quality factor resonant structures. Perovskite photonic crystals,[122,123] with the ability to enhance scintillation, or metasurfaces with lensing behavior[124] can be fabricated through cost-efficient and scalable methods such as thermal nanoimprint and soft lithography.[11] Another strategy exploits the multilayered deposition of MPHs and/or MCs, resulting in heterostructures and Bragg stacks.[125,126] In a recent study, coupling perovskite thin film emitters to a plasmonic layer resulted in over twofold enhancement of the scintillation intensity, as well as faster emission and improved x-ray imaging resolution.[83] Such thin film plasmonic/perovskite heterostructures with their scalable area are thus also promising for nuclear battery applications and can be further developed into perovskite/plasmonic metasurfaces with new functionalities. Alternatively, low self-absorption bulk perovskite–polymer composites with plasmonic enhancement are being developed,[127] which are extremely interesting for thickness scaling of the scintillating layer, resulting in stronger intensity of scintillation light. By integrating low-loss perovskite materials with nanophotonic and plasmonic components to create multilayer scintillation devices with substantial thickness, one can potentially achieve high stopping power, significant Purcell enhancements, and efficient light extraction.[11] Finally, there is also an attempt to confine high-energy photons, such as x-rays and gamma rays, within nanostructures in diamonds.[128] This technique has the potential to enhance the efficiency of not only radiovoltaic devices but also radio-PV systems.[129] The successfully demonstrated concepts of photonic and plasmonic enhancement in the field of scintillator research pave the way for the adoption of similar photonics- and plasmonic-based strategies in the development of highly efficient nuclear batteries.

VII. CHALLENGES AND LIMITATIONS

MPHs and MCs exhibit exceptional optoelectronic properties, such as high absorption coefficients and tunable bandgaps, which are vital for enhancing PCE in non-thermal conversion scheme.[104,130,131]

In thermal conversion nuclear batteries, where heat from radioactive decay is converted into electricity, MCs, particularly telluride-based compounds, have shown significant potential due to their outstanding thermoelectric properties and high thermal stability. However, the future application of MPHs and MCs in nuclear battery solutions requires thorough analysis of fundamental limitation factors, engineering risks, and technical difficulties regarding these materials. Their successful implementation in RVBs and RPVBs depends on the development of improved synthesis techniques or formulas, focusing on the issues of durability, stability, and scalability.

A. Key limitation factors for practical implementation of MPHs and MCs in nuclear batteries

As mentioned in Secs. IV and V, the MHPs suffer from low stability of their crystal structure, which makes them vulnerable to environmental conditions, such as oxygen and moisture. Thus, in practical realizations of such devices, one needs to consider encapsulation strategies, as to isolate the perovskite film from the harmful factors. The risk of lattice degradation caused by high energy particles is also significant and may lead to rapid deterioration of MPHs-based nuclear batteries over time. For this reason, implementing MPHs in nuclear batteries will likely require lower activity sources than in-state-of-the-art materials. Currently, the vulnerability of MPHs to high energy particles limits their application to β-voltaics. Alpha α radiation sources seem impractical now, but there is potential use in harvesting energy from γ-photons. In the case of MCs, the environmental stability and radiation hardness can be much higher than for MPHs; however, it comes with a cost of more challenging growth techniques, often requiring sophisticated methods such as chemical vapor deposition (CVD). Another major limitation comes from the self-absorption of emitted radiation, which can be relatively high in MPHs used for scintillating components in RPVBs and the same applies to MCs, such as ZnS:Cu. Self-absorption can become a significant problem if the required thickness of the scintillating film (the probability of particle absorption, as well as the emitted power scales with thickness) is more than 100 μm.[130]

B. Challenges for future development of MPHs- and MCs-based nuclear batteries

The above-mentioned limitation factors in MPHs highlight the need for further advancements in material composition with the focus on low-dimensional crystal structures, such as 2D, 1D, 0D, or mixed.[132] Perovskite low dimensional materials often present higher Stokes shift than their 3D counterparts, increased structural stability, and reduced ion migration. However, they can be also more challenging when it comes to growth techniques. The precise engineering required to optimize the bandgap and refractive index of MPHs also complicates large-scale production, potentially increasing costs and hindering widespread adoption. In general, the solution-based growth techniques used for MPHs are relatively cost efficient, but the variations of the material properties from batch to batch might be a serious obstacle in the development of final product. Moreover, although perovskite halides have demonstrated impressive scintillation light yields,[9] there is currently no established benchmark for scintillation techniques in nuclear batteries.

In the case of MCs and their application in thermal conversion schemes, achieving high PD remains a considerable challenge due to the trade-offs between electrical conductivity and thermal conductivity in thermoelectric materials. Although advances in nanostructuring and doping have improved the performance of MCs, maintaining these improvements at elevated temperatures over extended periods remains difficult, leading to potential performance degradation. Additionally, the use of photonic enhancements, such as photonic crystals and plasmonic structures, to boost light outcoupling and emission rates introduces further complexity. These enhancements require precise fabrication techniques and careful design to prevent issues like increased optical losses or mechanical instability. Consequently, while photonic and plasmonic strategies offer significant theoretical advantages for nuclear battery performance, their practical application is currently constrained by existing manufacturing capabilities and the need for more durable and scalable solutions. Similarly, the impact of photonic and plasmonic enhancements on light generation for PV components remains underexplored, leaving a gap in understanding how much enhancement is necessary to achieve optimal performance.

VIII. OUTLOOK

The field of nuclear battery technology is on the cusp of transformative advancements, driven by the exploration of innovative materials like MPHs and MCs. These materials offer remarkable optoelectronic properties that have the potential to significantly enhance the efficiency and compactness of both radiovoltaic and thermoelectric nuclear batteries. MPHs, with their high absorption coefficients and tunable bandgaps, show promise in improving PCE in radiovoltaic systems. Despite these advantages, challenges such as sensitivity to moisture and radiation, coupled with issues like self-absorption and limited commercial readiness, need to be addressed to unlock their full potential. Similarly, MCs demonstrate excellent thermoelectric properties ideal for thermal nuclear batteries but face hurdles in achieving high power densities and maintaining performance at elevated temperatures. The integration of advanced photonic and plasmonic enhancements into these systems is expected to further push the boundaries of efficiency by improving light outcoupling and emission rates, though practical implementation remains constrained by current manufacturing capabilities and design complexities. Figure 6 shows all factors that are important in the development of state-of-the-art nuclear batteries. Within this corridor, this emerging technology could provide longevity and applicability of the low-dimensional materials such as MPHs and MCs for nuclear battery applications in coming years. As the main ingredient toward boosting, the efficiency and compactness has recently coming to the surface.

Looking ahead, a continue innovation and research are crucial to overcoming these challenges and realizing the full potential of MPHs and MCs in nuclear battery applications. Advances in materials science, such as improved stability of MPHs and enhanced thermoelectric properties of MCs, combined with state of the art photonic and plasmonic enhancements,[115] could drive the next generation of nuclear batteries, especially for high power modes (>mW). Other enhancement can be introduced by the confinement of the radioactive sources using diamond nanostructures.[128] These advancements hold the promise of expanding the applications of nuclear batteries from specialized uses in space exploration and defense to broader applications in medical devices and remote sensing. As the field progresses, a concerted effort to address the existing limitations and refine material

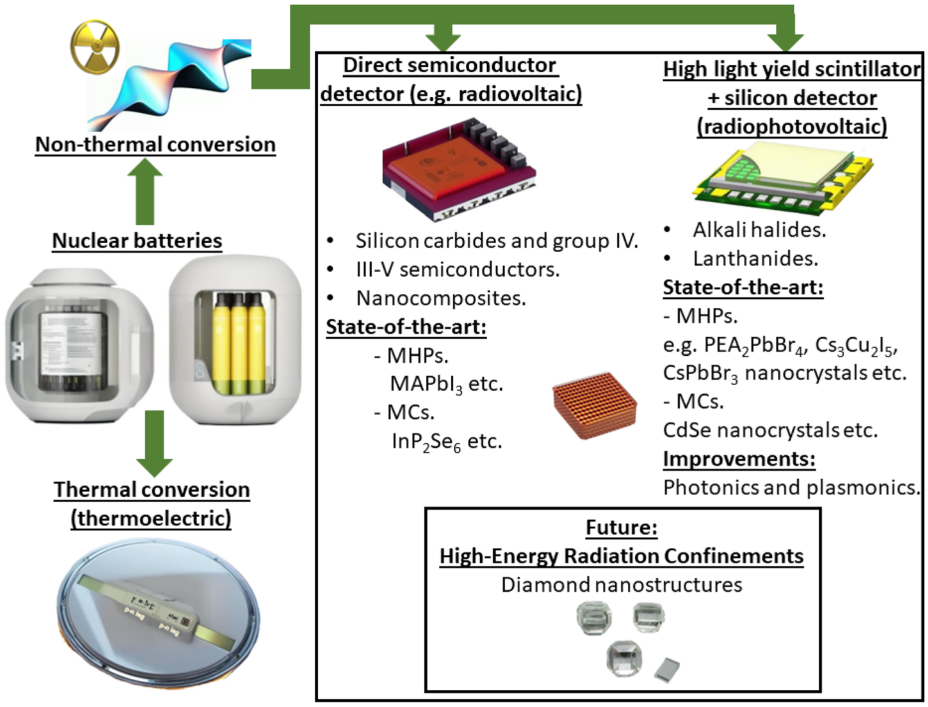

FIG. 6. Research roadmap of non-thermal conversion batteries and comparison with current thermal conversion batteries. The roadmap highlights advancements in both types of batteries, emphasizing significant progress in the efficiencies of halide and chalcogenide semiconductor and scintillator materials.

properties will be essential in achieving scalable, high-performance nuclear batteries that meet the demands of emerging technologies and applications.

ACKNOWLEDGMENTS

This work was supported by the National Science Center, Poland, under grant OPUS-24 No. 2022/47/B/ST5/01966.

AUTHOR DECLARATIONS

Conflict of Interest

The authors have no conflicts to disclose.

Author Contributions

D. Kowal: Validation (equal); Visualization (equal); Writing – original draft (equal). **S. Mahato:** Investigation (equal); Resources (equal); Validation (equal). **M. Makowski:** Formal analysis (equal); Resources (equal); Validation (equal). **S. Hartati:** Investigation (equal); Resources (equal); Validation (equal). **M. A. K. Sheikh:** Investigation (equal); Resources (equal); Writing – original draft (equal). **W. Ye:** Investigation (equal); Methodology (equal); Validation (equal). **D. R. Schaart:** Methodology (equal); Resources (equal); Validation (equal). **J. Cybinska:** Investigation (equal); Validation (equal); Writing – review & editing (equal). **L. J. Wong:** Methodology (equal); Resources (equal); Writing – review & editing (equal). **A. Arramel:** Conceptualization (equal); Investigation (equal); Supervision (equal); Validation (equal); Writing – review & editing (equal). **M. D. Birowosuto:** Conceptualization (equal); Data curation (equal); Funding acquisition (equal); Investigation (equal); Methodology (equal); Supervision (equal); Validation (equal); Writing – review & editing (equal).

DATA AVAILABILITY

Data sharing is not applicable to this article as no new data were created or analyzed in this study.

REFERENCES

[1] M. A. Prelas, C. L. Weaver, M. L. Watermann, E. D. Lukosi, R. J. Schott, and D. A. Wisniewski, "A review of nuclear batteries," Prog. Nucl. Energy **75**, 117–148 (2014).

[2] M. B. Naseem, H. S. Kim, J. Lee, C. H. Kim, and S.-I. In, "Betavoltaic nuclear battery: A review of recent progress and challenges as an alternative energy source," J. Phys. Chem. C **127**(16), 7565–7579 (2023).

[3] C. F. Bohren and D. R. Huffman, *Absorption and Scattering of Light by Small Particles* (John Wiley & Sons, 2008).

[4] C. Forsberg and A. W. Foss, "Fission battery markets and economic requirements," Appl. Energy **329**, 120266 (2023).

[5] C. Forsberg, A. Foss, and A. Abou-Jaoude, "Fission battery economics-by-design," Prog. Nucl. Energy **152**, 104366 (2022).

[6] H. Wei and J. Huang, "Halide lead perovskites for ionizing radiation detection," Nat. Commun. **10**, 1066 (2019).

[7] S. Johnsen, Z. Liu, J. A. Peters, J.-H. Song, S. C. Peter, C. D. Malliakas, N. K. Cho, H. Jin, A. J. Freeman, B. W. Wessels, and M. G. Kanatzidis, "Thallium chalcogenide-based wide-band-gap semiconductors: $TlGaSe_2$ for radiation detectors," Chem. Mater. **23**(12), 3120–3128 (2011).

[8] D. G. Chica, Y. He, K. M. McCall, D. Y. Chung, R. O. Pak, G. Trimarchi, Z. Liu, P. M. D. Lurgio, B. W. Wessels, and M. G. Kanatzidis, "Direct thermal neutron detection by the 2D semiconductor $^6LiInP_2Se_6$," Nature **577**, 346–349 (2020).

[9] M. D. Birowosuto, D. Cortecchia, W. Drozdowski, K. Brylew, W. Lachmanski, A. Bruno, and C. Soci, "X-ray scintillation in lead halide perovskite crystals," Sci. Rep. **6**, 37254 (2016).

[10] Q. Chen, J. Wu, X. Ou, B. Huang, J. Almutlaq, A. A. Zhumekenov, X. Guan, S. Han, L. Liang, Z. Yi, J. Li, X. Xie, Y. Wang, Y. Li, D. Fan, D. B. L. Teh, A. H. All, O. F. Mohammed, O. M. Bakr, T. Wu, M. Bettinelli, H. Yang, W. Huang, and X. Liu, "All-inorganic perovskite nanocrystal scintillators," Nature **561**, 88–93 (2018).

[11] F. Maddalena, L. Tjahjana, A. Z. Xie, S. W. Zeng, H. Wang, P. Coquet, W. Drozdowski, C. Dujardin, C. Dang, and M. D. Birowosuto, "Inorganic, organic, and perovskite halides with nanotechnology for high–light yield X- and γ-ray scintillators," Crystals **9**(2), 88 (2019).

[12] S. E. Létant and T.-F. Wang, "Study of porous glass doped with quantum dots or laser dyes under alpha irradiation," Appl. Phys. Lett **88**(10), 103110 (2006).

[13] S. E. Létant and T.-F. Wang, "Semiconductor quantum dot scintillation under gamma-ray irradiation," Nano Lett. **6**(12), 2877–2880 (2006).

[14] C. Liu, Z. Li, T. J. Hajagos, D. Kishpaugh, D. Y. CHen, and Q. Pei, "Transparent ultra-high-loading quantum dot/polymer nanocomposite monolith for gamma scintillation," ACS Nano **11**(6), 6422–6430 (2017).

[15] S. Y. F. Chu, L. P. Ekstrom, and R. B. Firestone, "The Lund/LBNL nuclear data search," (1999). accessed June 27, 2024.

[16] National_Research_Council_Radioisotope_Power_Systems_Committee, *Radioisotope Power Systems: An Imperative for Maintaining US Leadership in Space Exploration* (National Academies Press, 2009).

[17] B. C. Blanke, J. H. Birden, K. C. Jordan, and E. L. Murphy, *Nuclear Battery-Thermocouple Type Summary Report* (Department of Commerce, 1962).

[18] F. Ritz and C. E. Peterson, "Multi-mission radioisotope thermoelectric generator (MMRTG) program overview," IEEE Aerosp. Conf. Proc. **2957**(5), 2950–2957 (2004).

[19] G. N. Hatsopoulos and E. P. Gyftopoulos, *Thermionic Energy Conversion: Processes and Devices* (MIT Press, 1973).

[20] C. J. Eiting, V. Krishnamoorthy, S. Rodgers, T. George, J. D. Robertson, and J. Brockman, "Demonstration of a radiation resistant, high efficiency SiC betavoltaic," Appl. Phys. Lett. **88**, 064101 (2006).

[21] D.-Y. Qiao, X.-J. Chen, Y. Ren, and W.-Z. Yuan, "A micro nuclear battery based on SiC Schottky barrier diode," JMEMS **20**, 658–690 (2011).

[22] C. Thomas, S. Portnoff, and M. G. Spencer, "High efficiency 4H-SiC betavoltaic power sources using tritium radioisotopes," Appl. Phys. Lett **108**(1), 013505 (2016).

[23] V. Bormashov, S. Troschiev, A. Volkov, S. Tarelkin, E. Korostylev, A. Golovanov, M. Kuznetsov, D. Teteruk, N. Kornilov, S. Terentiev, S. Buga, and V. Blank, "Development of nuclear microbattery prototype based on Schottky barrier diamond diodes," Phys. Status Solidi (a) **212**(11), 2539–2548 (2015).

[24] S. Aydin and E. Kam, "Investigation of nickel-63 radioisotope-powered GaN betavoltaic nuclear battery," Int. J. Energy Res. **43**(14), 8725–8738 (2019).

[25] X. Guo, Y. Liu, Z. Xu, Z. Jin, K. Liu, Z. Yuan, P. Gong, and X. Tang, "Multi-level radioisotope batteries based on ^{60}Co γ source and radio-voltaic/radio-photovoltaic dual effects," Sens. Actuators A Phys. **275**, 119–128 (2018).

[26] L. C. Olsen, "Betavoltaic energy conversion," Energy Convers. **13**(4), 117–127 (1973).

[27] S. I. Maximenko, J. E. Moore, C. A. Affouda, and P. P. Jenkins, "Optimal semiconductors for ^{3}H and ^{63}Ni betavoltaics," Sci. Rep. **9**(1), 10892 (2019).

[28] M. L. Terranova, "Nuclear batteries: Current context and near-term expectations," Int. J. Energy Res. **46**(14), 19368–19393 (2022).

[29] M. Kosfeld, B. Westphal, and A. Kwade, "Moisture behavior of lithium-ion battery components along the production process," J. Energy Storage **57**, 106174 (2023).

[30] B. C. Blanke, J. H. Birden, K. C. Jordan, and E. L. Murphy, *Nuclear Battery-Thermocouple Type Summary Report* (United States Atomic Energy Commission, 1960).

[31] *General Safety Considerations* (Fusion Technology Institute, University of Wisconsin–Madison, 2000).

[32] "Thirty-one years of clinical experience with "nuclear-powered" in pacemakers—PARSONNET," in *Pacing and Clinical Electrophysiology* (Wiley Online Library, 2006).

[33] M. M. A. Gamel, H. J. Lee, W. E. S. W. A. Rashid, P. J. Ker, L. K. Yau, M. A. Hannan, and M. Z. Jamaludin, "A review on thermophotovoltaic cell and its applications in energy conversion: Issues and recommendations," Materials **14**(17), 4944 (2021).

[34] Z. Omair, G. Scranton, L. M. Pazos-Outón, T. P. Xiao, M. A. Steiner, V. Ganapati, P. F. Peterson, J. Holzrichter, H. Atwater, and E. Yablonovitch, "Ultraefficient thermophotovoltaic power conversion by band-edge spectral filtering," Proc. Natl. Acad. Sci. U. S. A. **116**(31), 15356–15361 (2019).

[35] P. Rappaport, "The electron-voltaic effect in p-n junctions induced by beta-particle bombardment," Phys. Rev. **93**(1), 246–247 (1954).

[36] L. C. Olsen, "Advanced betavoltaic power sources," in *Proceedings of the 9th Intersociety Energy Conversion Engineering Conference*, edited by A. R. Liberman and W. E. Osmeyer (American Society of Mechanical Engineers, New York, 1974), pp. 754–762.

[37] M. V. S. Chandrashekhar, C. I. Thomas, H. Li, M. G. Spencer, and A. Lal, "Demonstration of a ^{4}H SiC betavoltaic cell," Appl. Phys. Lett. **88**, 033506 (2006).

[38] R. Zheng, J. Lu, Y. Wang, Z. Chen, X. Zhang, X. Li, L. Liang, L. Qin, Y. Zeng, Y. Chen, and Y. Liu, "Understanding efficiency improvements of betavoltaic batteries based on ^{4}H-SiC, GaN, and diamond," Appl. Phys. Lett. **121**, 103902 (2022).

[39] L. Zhang, H.-L. Cheng, X.-C. Hu, and X.-B. Xu, "Model and optimal design of ^{147}Pm SiC-based betavoltaic cell," Superlattices Microstruct. **123**, 60–70 (2018).

[40] J. W. Murphy, C. D. Frye, R. A. Henderson, M. A. Stoyer, L. F. Voss, and R. J. Nikolic, "Demonstration of a three-dimensionally structured betavoltaic," J. Elec. Mater. **50**, 1380–1385 (2021).

[41] G. Rybicki, C. Vargas-Aburto, and R. Uribe, "Silicon carbide alphavoltaic battery," in *Materials Science, Physics, Engineering: Conference Record of the Twenty Fifth IEEE Photovoltaic Specialists Conference* (IEEE, Washington, DC, 1996), pp. 93–96.

[42] R. Gao, L. Liu, Y. Li, L. Shen, P. Wan, X. Ouyang, H. Zhang, J. Ruan, L. Zhou, L. Chen, X. Zhang, J. Liu, H. Li, M. Liu, and X. Ouyang, "High-performance alpha-voltaic cell based on a ^{4}H-SiC PIN junction diode," Energy Convers. Manag. **252**, 115090 (2022).

[43] W. Ma, L. Liu, R. Gao, R. Jia, and X. Ouyang, "Radiation hardness characteristics of self-powered detector based on SiC/Si heterojunction diode," Sens. Actuator A Phys. **361**, 114563 (2023).

[44] B. Liu, K. Liu, J. Zhao, W. Wang, V. Ralchenko, F. Geng, L. Yang, S. Zhang, J. Xue, J. Han, J. Zhu, and B. Dai, "Enhanced performance of diamond Schottky nuclear batteries by using ZnO as electron transport layer," Diam. Relat. Mater. **109**, 108026 (2020).

[45] J. Xue, Q. Hou, L. Niu, Z. Ma, Y. Shi, J. Tang, and J. Liu, "Silicon substrate diamond film detector for gamma dose rate measurement in a high radiation environment," Diam. Relat. Mater. **121**, 108752 (2022).

[46] T. Shimaoka, H. Umezawa, K. Ichikawa, J. Pernot, and S. Koizumi, "Ultrahigh conversion efficiency of betavoltaic cell using diamond pn junction," Appl. Phys. Lett. **117**(10), 103902 (2020).

[47] G. R. Mackenzie, S. Kaluvan, P. G. Martin, C. Hutson, T. Connolley, M. Cattelan, H. Dominguez-Andrade, T. L. Martin, N. A. Fox, and T. B. Scott, "A diamond gammavoltaic cell utilizing surface conductivity and its response to different photon interaction mechanisms," Mater. Today Energy **21**, 100688 (2021).

[48] M. Lu, G.-G. Zhang, K. Fu, G. Yu, D. Su, and J. Hu, "Gallium nitride schottky betavoltaic nuclear batteries," Energy Convers. Manag. **52**, 1955–1958 (2011).

[49] Z. J. Cheng, H. S. San, Z. H. Feng, B. Liu, and X. Y. Chen, "High open-circuit voltage betavoltaic cell based on GaN pin homojunction," Electron. Lett. **47**, 720–722 (2011).

[50] H. San, S. Yao, X. Wang, Z. Cheng, and X. Chen, "Design and simulation of GaN based Schottky betavoltaic nuclear micro-battery," Appl. Radiat. Isot. **80**, 17–22 (2013).

[51] F. H. Li, X. Gao, Y. L. Yuan, J. S. Yuan, and M. Lu, "GaN PIN betavoltaic nuclear batteries," Sci. China Technol. Sci. **57**, 25–28 (2014).

[52] D.-S. Kim, Y. J. Yoon, J. S. Lee, I. M. Kang, and J.-H. Lee, "Experimental and simulation study of power performance improvement of GaN PIN betavoltaic cell," Intl. J. Energy Res. **45**, 17622–17630 (2021).

[53] Z. Chen, R. Zheng, J. Lu, X. Li, Y. Wang, X. Zhang, Y. Zhang, X. Yuan, Q. Cui, Y. Zhao, and H. Li, "Modeling and optimization of GaN-based

betavoltaic batteries: Comparison of p-n and p-i-n junctions," AIP Adv. **12**, 085112 (2022).

[54] R. Gao, L. Liu, X. Xia, P. Wan, X. Ouyang, W. Ma, X. Geng, H. Wang, R. Xu, K. Zhang, H. Liang, and X. Ouyang, "Isoelectronic aluminum-doped gallium nitride alpha-voltaic cell with efficiency exceeding 4.5%," Commun. Mater. **4**, 50 51–58 (2023).

[55] W. Sun, N. P. Kherani, K. D. Hirschman, L. L. Gadeken, and P. M. Fauchet, "A three-dimensional porous silicon p–n diode for betavoltaics and photovoltaics," Adv. Mater. **17**, 1230–1233 (2005).

[56] Q. Zhang, R. Chen, H. San, G. Liu, and K. Wang, "Betavoltaic effect in titanium dioxide nanotube arrays under build-in potential difference," J. Power Sources **282**, 529–533 (2015).

[57] G. K. Mor, O. K. Varghese, M. Paulose, K. Shankar, and C. A. Grimes, "A review on highly ordered, vertically oriented TiO$_2$ nanotube arrays: Fabrication, material properties, and solar energy applications," Sol. Energy Mat. Sol. C **90**, 2011–2075 (2006).

[58] C. Chen, N. Wang, P. Zhou, H. San, K. Wang, and X. Chen, "Electrochemically reduced graphene oxide on well-aligned titanium dioxide nanotube arrays for betavoltaic enhancement," ACS Appl. Mater. Interfaces **8**, 24638–24644 (2016).

[59] C. Chen, J. Chen, Z. Wang, J. Zhang, H. San, S. Liu, C. Wu, and W. Hofmann, "Free-standing ZnO nanorod arrays modified with single-walled carbon nanotubes for betavoltaics and photovoltaics," J. Mater. Sci. Technol. **54**, 48–57 (2020).

[60] N. Wang, R. Zheng, T. Chi, T. Jiang, Z. Ding, X. Li, S. Liu, L. Zhang, and H. San, "Betavoltaic-powered electrochemical cells using TiO$_2$ nanotube arrays incorporated with carbon nanotubes," Compos. B. Eng. **239**, 109952 (2022).

[61] Y. Hwang, Y. H. Park, H. S. Kim, D. H. Kim, S. Ali, S. Sorcar, M. C. Flores, M. R. Hoffmann, and S.-I. In, "C-14 powered dye-sensitized betavoltaic cells," Chem. Commun. **56**, 7080–7083 (2020).

[62] M. Sychov, A. Kavetsky, G. Yakubova, G. Walter, S. Yousaf, Q. Lin, D. Chan, H. Socarras, and K. Bower, "Alpha indirect conversion radioisotope power source," Appl. Radiat. Isot. **66**, 173–177 (2008).

[63] L. Hong, X.-B. Tang, Z.-H. Xu, Y.-P. Liu, and D. Chen, "Radioluminescent nuclear batteries with different phosphor layers," Nucl. Instrum. Methods Phys. Res. B **338**, 112–118 (2014).

[64] Z. Xu, X. Tang, Y. Liu, Z. Zhang, W. Chen, Z. Yuan, and K. Liu, "ZnS:Cu phosphor layers as energy conversion materials for nuclear batteries: A combined theoretical and experimental study of their geometric structure," Energy Technol. **5**, 1638–1646 (2017).

[65] T. Jiang, Z. Ding, R. Zheng, X. Tang, Z. Xu, X. Li, L. Zhang, X. Li, and H. San, "^{63}Ni-based radioluminescent isotope cells with enhanced photon transport interfaces," J. Sci.-Adv. Mater. Dev. **8**(3), 100611 (2023).

[66] Y. He, Z. Xu, H. Wang, M. Bian, Y. Liu, and X. Tang, "Enhanced radioluminescence and improved radioluminescent nuclear battery output performance more than 50% with SiO$_2$ nanosphere coating," J. Lumin. **255**, 119600 (2023).

[67] S. Xue, C. Tan, P. Kandlakunta, I. Oksuz, V. Hlinka, and L. R. Cao, "Methods for improving the power conversion efficiency of nuclear-voltaic batteries," Nucl. Instrum. Methods Phys. Res. A **927**, 133–139 (2019).

[68] Z.-R. Zhang, X.-B. Tang, Y.-P. Liu, Z.-H. Xu, Z.-C. Yuan, K. Liu, and W. Chen, "GaAs radiovoltaic cell enhanced by Y$_2$SiO$_5$ crystal for the development of new gamma microbatteries," Nucl. Instrum. Methods Phys. Res. B **398**, 35–41 (2017).

[69] A. Toor, A. Wen, F. Maksimovic, A. M. Gaikwad, K. S. J. Pister, and A. C. Arias, "Stencil-printed Lithium-ion micro batteries for IoT applications," Nano Energy **82**, 105666 (2021).

[70] H.-J. He, Y.-C. Han, X.-Y. Wang, Y.-M. Liu, J.-C. Zhang, L. Ren, and M.-J. Zheng, "Enhancing betavoltaic nuclear battery performance with 3D P$^+$PNN$^+$ multi-groove structure via carrier evolution," Nucl. Sci. Technol. **34**, 180–196 (2023).

[71] A. Ghorai, S. Mahato, S. Singh, S. Bose, B. Roy, U. Jeong, and S. K. Ray, "Ligand-mediated revival of degraded A-CsPbI$_3$ to stable highly luminescent perovskite," Angew. Chem. **62**(22), e202302852 (2023).

[72] M. A. K. Sheikh, F. Maddalena, D. Kowal, M. Makowski, S. Mahato, R. Jędrzejewski, R. Bhattarai, M. E. Witkowski, K. J. Drozdowski, W. Drozdowski, C. Dang, T. D. Rhone, and M. D. Birowosuto, "Effect of dual-organic cations on the structure and properties of 2D hybrid perovskites as scintillators," ACS Appl. Mater. Interfaces **16**(19), 25529–25539 (2024).

[73] S. Mahato, A. Ghorai, S. K. Srivastava, M. Modak, S. Singh, and S. K. Ray, "Highly air-stable single-crystalline β-CsPbI$_3$ nanorods: A platform for inverted perovskite solar cells," Adv. Energy Mater. **10**(30), 2001305 (2020).

[74] S. Mahato, M. Tamulewicz-Szwajkowska, S. Singh, D. Kowal, S. Bose, J. Serafińczuk, K. Czyż, R. Jędrzejewski, M. D. Birowosuto, S. K. Ray, and A. L. Abdelhady, "Surface-engineered methylammonium lead bromide single crystals: A platform for fluorescent security tags and photodetector applications," Adv. Opt. Mater. **12**(10), 2302257 (2024).

[75] S. Mahato, M. Makowski, S. Bose, D. Kowal, M. A. K. Sheikh, P. Braueninger-Wemer, M. E. Witkowski, S. K. Ray, W. Drozdowski, and M. D. Birowosuto, "Improvement of light output of MAPbBr$_3$ single crystal for ultrafast and bright cryogenic scintillator," J. Phys. Chem. Lett. **15**(14), 3713–3720 (2024).

[76] S. Ghosh, S. Mishra, and T. Singh, "Antisolvents in perovskite solar cells: Importance, issues, and alternatives," Adv. Mater. Interfaces **7**(18), 2000950 (2020).

[77] F. Maddalena, M. H. Mahyuddin, D. Kowal, M. E. Witkowski, M. Makowski, M. A. K. Sheikh, S. Mahato, R. Je˛drzejewski, W. Drozdowski, C. Dujardin, C. Dang, and M. D. Birowosuto, "Lattice expansion in rubidium doped hybrid organic-inorganic perovskite crystals resulting smaller-bandgap and higher-light-yield scintillators," Inorg. Chem. **62**, 8892–8902 (2023).

[78] A. Mandal, S. K. Khuntia, D. Mondal, P. Mahadevan, and S. Bhattacharyya, "Spin texture sensitive photodetection by Dion-Jacobson tin halide perovskites," J. Am. Chem. Soc. **145**(45), 24990–25002 (2023).

[79] M. A. K. Sheikh, D. Kowal, M. H. Mahyuddin, R. Cala', E. Auffray, M. E. Witkowski, M. Makowski, W. Drozdowski, H. Wang, C. Dujardin, D. Cortecchia, and M. D. Birowosuto, "A$_2$B$_{n-1}$Pb$_n$I$_{3n+1}$ (A = BA, PEA; B = MA; n = 1, 2): Engineering quantum-well crystals for high mass density and fast scintillators," J. Phys. Chem. C **127**(22), 10737–10747 (2023).

[80] A. Wibowo, M. A. K. Sheikh, L. J. Diguna, M. B. Ananda, M. A. Marsudi, A. Arramel, S. Zeng, L. J. Wong, and M. D. Birowosuto, "Development and challenges in perovskite scintillators for high resolution imaging, and timing applications," Commun. Mater. **4**(21), 1–10 (2023).

[81] S. Pal, A. Ghorai, S. Mahato, and S. K. Ray, "Piezo-phototronic effect-induced self-powered broadband photodetectors using environmentally stable α-CsPbI$_3$ perovskite nanocrystals," Adv. Opt. Mater **11**(16), 2300233 (2023).

[82] B. Guzelturk, B. T. Diroll, J. P. Cassidy, D. Harankahage, M. Hua, X.-M. Lin, V. Iyer, R. D. Schaller, B. J. Lawrie, and M. Zamkov, "Bright and durable scintillation from colloidal quantum shells," Nat. Commun. **15**, 4274 (2024).

[83] W. Ye, Z. Yong, M. Go, D. Kowal, F. Maddalena, L. Tjahjana, H. Wang, A. Arramel, C. Dujardin, M. D. Birowosuto, and L. J. Wong, "The nanoplasmonic purcell effect in ultrafast and high-light-yield perovskite scintillators," Adv. Mater. **36**(25), e2309410 (2024).

[84] H. Wei, Y. Fang, P. Mulligan, W. Chuirazzi, H.-H. Fang, C. Wang, B. R. Ecker, Y. Gao, M. A. Loi, L. Cao, and J. Huang, "Sensitive X-ray detectors made of methylammonium lead tribromide perovskite single crystals," Nat. Photonics **10**, 333–339 (2016).

[85] B. Yang, L. Yin, G. Niu, J.-H. Yuan, K.-H. Xue, Z. Tan, X.-S. Miao, M. Niu, X. Du, H. Song, E. Lifshitz, and J. Tang, "Lead-free halide Rb$_2$CuBr$_3$ as sensitive X-ray scintillator," Adv. Mater. **31**, 1904711 (2019).

[86] S. Yakunin, M. Sytnyk, D. Kriegner, S. Shrestha, M. Richter, G. J. Matt, H. Azimi, C. J. Brabec, J. Stangl, M. V. Kovalenko, and W. Heiss, "Detection of X-ray photons by solution-processed lead halide perovskites," Nat. Photonics **9**, 444–449 (2015).

[87] W. Zhu, W. Ma, Y. Su, Z. Chen, X. Chen, Y. Ma, L. Bai, W. Xiao, T. Liu, H. Zhu, X. Liu, H. Liu, X. Liu, and Y. Yang, "Low-dose real-time X-ray imaging with nontoxic double perovskite scintillators," Light. Sci. Appl. **9**, 112 (2020).

[88] K. Song, L. Liu, D. Zhang, M. P. Hautzinger, S. Jin, and Y. Han, "Atomic-resolution imaging of halide perovskites using electron microscopy," Adv. Energy Mater. **10**(26), 1904006 (2020).

[89] S. Bose, S. Mahato, B. Roy, T. Singha, S. K. Srivastava, and S. K. Ray, "Unveiling electron dose-induced phase decomposition and energy kinetics in Cu-doped CsPbI$_3$ nanocrystals," ACS Appl. Nano Mater. **7**(6), 6020–6028 (2024).

[90] A. R. Kirmani, T. A. Byers, Z. Ni, K. VanSant, D. K. Saini, R. Scheidt, X. Zheng, T. B. Kum, I. R. Sellers, L. McMillon-Brown, J. Huang, B. Rout, and J.

M. Luther, "Unraveling radiation damage and healing mechanisms in halide perovskites using energy-tuned dual irradiation dosing," Nat. Commun. **15**(1), 696 (2024).

[91]M. L. Zaffalon, F. Cova, M. Liu, A. Cemmi, I. Di Sarcina, F. Rossi, F. Carulli, A. Erroi, C. Rodà, J. Perego, A. Comotti, M. Fasoli, F. Meinardi, L. Li, A. Vedda, and S. Brovelli, "Extreme γ-ray radiation hardness and high scintillation yield in perovskite nanocrystals," Nat. Photonics **16**(12), 860–868 (2022).

[92]Z. Song, C. Zhao, F. Liao, and Y. Zhao, "Perovskite-betavoltaic cells: A novel application of organic-inorganic hybrid halide perovskites," ACS Appl. Mater. Interfaces **11**, 32969–33297 (2019).

[93]R. Gao, R. Chen, P. Wan, X. Ouyang, Q. Lei, Q. Deng, X. Guan, G. Niu, J. Tang, W. Chen, Z. Liu, X. Ouyang, and L. Liu, "High efficiency formamidinium-cesium perovskite-based radio-photovoltaic cells," Energy Environ. Mater. **7**, e12513 (2022).

[94]G. Li, C. Zhao, Y. Liu, J. Ren, Z. Zhang, H. Di, W. Jiang, J. Mei, and Y. Zhao, "High-performance perovskite betavoltaics employing high-crystallinity $MAPbBr_3$ films," ACS Omega **6**, 20015–20025 (2021).

[95]X. Li, J. Chen, D. Yang, X. Chen, D. Geng, L. Jiang, Y. Wu, C. Meng, and H. Zeng, "Mn^{2+} induced significant improvement and robust stability of radioluminescence in $Cs_3Cu_2I_5$ for high-performance nuclear battery," Nat. Commun. **12**, 3879 (2021).

[96]Z. Xu, X. Tang, Y. Liu, Z. Zhang, W. Chen, K. Liu, and Z. Yuan, "$CsPbBr_3$ quantum dot films with high luminescence efficiency and irradiation stability for radioluminescent nuclear battery application," ACS Appl. Mater. Interfaces **11**(15), 14191–14199 (2019).

[97]R. Gao, X. Ouyang, Q. Wang, P. Wan, W. Ma, X. Du, Y. Wu, L. Liu, and X. Ouyang, "High performance radioluminescent nuclear battery based on ultrabright $Cs_3Cu_2I_5$:Tl single crystal scintillator," IEEE Trans. Nucl. Sci. **71**, 2530–2535 (2024).

[98]K. Li, C. Yan, J. Wang, K. Zhu, J. Guo, Y. Zhang, G. Shi, Y. Yin, L. Cheng, L. Sun, Y. Wang, H. Zhang, Y. Sun, J. Yuan, W. Ma, G. Ji, Z. Chai, Y. Wang, X. Ouyang, and S. Wang, "Micronuclear battery based on a coalescent energy transducer," Nature **633**(8031), 811–815 (2024).

[99]D. Yang, Z. Xu, C. Gong, L. Su, X. Li, X. Tang, D. Geng, C. Meng, F. Xu, and H. Zeng, "Armor-like passivated $CsPbBr_3$ quantum dots: Boosted stability with hand-in-hand ligands and enhanced performance of nuclear batteries," J. Mater. Chem. A **9**, 8772–8781 (2021).

[100]A. Assoud, N. Soheilnia, and H. Kleinke, "Thermoelectric properties of the new tellurides $SrSc_2Te_4$ and $BaSc_2Te_4$ in comparison to BaY_2Te_4," Intermetallics **15**(3), 371–376 (2007).

[101]A. Salah Mohamed, B. Gul, M. Salman Khan, B. Ahmad, G. Benabdellah, and H. Ahmad, "Predictive modeling of novel $GaAgX_2$ (X = S, Se) chalcogenides: First-principles study of electronic, optical, and thermoelectric properties," Chem. Phys. Lett. **846**, 141326 (2024).

[102]M. Jawad, A. U. Rahman, Q. Rafique, S. Azam, and F. Ijaz, "First principle investigation of structural, electronic, optical and thermoelectric properties of Chalcogenide Sr_2GeX_4 (X = S, Se)," Mater. Sci. Semicond. Process. **173**, 108105 (2024).

[103]M. S. Khan, B. Gul, H. Ahmad, A. S. Mohamed, S. M. Aziz, and F. Abbas, "First-principles study of the electronic structure, optical, and thermoelectric properties of novel WSeX (X = S, Te) chalcogenides: For energy harvesting application," Chem. Phys. Lett. **853**, 141523 (2024).

[104]S. Puthran, G. S. Hegde, and A. N. Prabhu, "Review of chalcogenide-based materials for low-, mid-, and high-temperature thermoelectric applications," J. Electron. Mater. **53**, 5739 (2024).

[105]N. Thakur, K. A. Aly, M. Mohery, M. M. Ebrahium, P. Kumar, and P. Sharma, "Recent advances in $BaZrS_3$ perovskites: Synthesis, properties, and future trends," J. Alloys Compd. **957**, 170457 (2023).

[106]J. Zheng, M. Ma, G. Yang, Y. Wu, and D. Mei, "Progress in the study of binary chalcogenide-based thermoelectric compounds," J. Solid State Chem. **334**, 124617 (2024).

[107]P. Sun, B. Wei, J. Zhang, J. M. Tomczak, A. M. Strydom, M. Søndergaard, B. B. Iversen, and F. Steglich, "Large Seebeck effect by charge-mobility engineering," Nat. Commun. **6**, 7475 (2015).

[108]T. Park, H. Lim, J. U. Hwang, J. Na, H. Lee, and E. Kim, "Roll type conducting polymer legs for rigid-flexible thermoelectric generator," APL Mater. **5**(7), 074106 (2017).

[109]Z. Yuan, X. Tang, Y. Liu, Z. Xu, K. Liu, J. Li, Z. Zhang, and H. Wang, "Improving the performance of a screen-printed micro-radioisotope thermoelectric generator through stacking integration," J. Power Sources **414**, 509–516 (2019).

[110]S. Lin, S. Xie, Y. Lei, T. Gan, L. Wu, J. Zhang, and Y. Yang, "Betavoltaic battery prepared by using polycrystalline CdTe as absorption layer," Opt. Mater. **127**, 112265 (2022).

[111]Z. Xu, Y. Liu, and X. Tang, "Radioluminescent nuclear battery technology development for space exploration," Adv. Astronaut. Sci. Technol. **3**(2), 125–131 (2020).

[112]Z. Yu, X. Wei, Y. Zheng, H. Hui, M. Bian, S. Dhole, J. H. Seo, Y. Y. Sun, Q. Jia, S. Zhang, S. Yang, and H. Zeng, "Chalcogenide perovskite $BaZrS_3$ thin-film electronic and optoelectronic devices by low temperature processing," Nano Energy **85**, 105959 (2021).

[113]E. N. V. Mercy, D. Srinivasan, and L. Marasamy, "Emerging $BaZrS_3$ and $Ba(Zr,Ti)S_3$ chalcogenide perovskite solar cells: A numerical approach toward device engineering and unlocking efficiency," ACS Omega **9**(4), 4359–4376 (2024).

[114]A. A. Pradhan, M. C. Uible, S. Agarwal, J. W. Turnley, S. Khandelwal, J. M. Peterson, D. D. Blach, R. N. Swope, L. Huang, S. C. Bart, and R. Agrawal, "Synthesis of $BaZrS_3$ and $BaHfS_3$ chalcogenide perovskite films using single-phase molecular precursors at moderate temperatures," Angew. Chem. Int. Ed. Engl. **62**(15), e202301049 (2023).

[115]H. C. Delgado, P. Moradifar, G. Chinn, C. S. Levin, and J. A. Dionne, "Toward "super-scintillation" with nanomaterials and nanophotonics," Nanophotonics **13**(11), 1953–1962 (2024).

[116]E. M. Purcell, "Spontaneous emission probabilities at radio frequencies," Phys. Rev. **69**, 37 (1946).

[117]C. Roques-Carmes, N. Rivera, A. Ghorashi, S. E. Kooi, Y. Yang, Z. Lin, J. Beroz, A. Massuda, J. Sloan, N. Romeo, Y. Yu, J. D. Joannopoulos, I. Kaminer, S. G. Johnson, and M. Soljačić, "A framework for scintillation in nanophotonics," Science **375**(6583), eabm9293 (2022).

[118]M. Salomoni, R. Pots, E. Auffray, and P. Lecoq, "Enhancing light extraction of inorganic scintillators using photonic crystals," Crystals **8**(2), 78 (2018).

[119]X. Chen, B. Liu, Q. Wu, Z. Zhu, J. Zhu, M. Gu, H. Chen, J. Liu, L. Chen, and X. Ouyang, "Enhanced light extraction of plastic scintillator using large-area photonic crystal structures fabricated by hot embossing," Opt. Express **26**(9), 11438–11446 (2018).

[120]Y. Kurman, A. Shultzman, O. Segal, A. Pick, and I. Kaminer, "Photonic-crystal scintillators: Molding the flow of light to enhance X-ray and γ-ray detection," Phys. Rev. Lett. **125**(4), 040801 (2020).

[121]Y. Kurman, N. Lahav, R. Schuetz, A. Shultzman, C. Roques-Carmes, A. Lifshits, S. Zaken, T. Lenkiewicz, R. Strassberg, O. Be'er, Y. Bekenstein, and I. Kaminer, "Purcell-enhanced x-ray scintillation," Sci. Adv. **10**(44), eadq6325 (2024).

[122]D. Kowal, L. J. Wong, and M. D. Birowosuto, "Large-area photonic bound state in the continuum for ultraviolet and deep-blue emission for organic, inorganic, and perovskite scintillators," IEEE Trans. Nucl. Sci. **70**(7), 1318–1324 (2023).

[123]S. Hou, A. Xie, Z. Xie, L. Y. M. Tobing, J. Zhou, L. Tjahjana, J. Yu, C. Hettiarachchi, D. Zhang, C. Dang, E. H. T. Teo, M. D. Birowosuto, and H. Wang, "Concurrent inhibition and redistribution of spontaneous emission from all inorganic perovskite photonic crystals," ACS Photonics **6**(6), 1331–1337 (2019).

[124]E. Klopfer, M. Lawrence, D. R. B. III, J. Dixon, and J. A. Dionne, "Dynamic focusing with high-quality-factor metalenses," Nano Lett. **20**(7), 5127–5132 (2020).

[125]P. Y. D. Maulida, S. Hartati, Y. Firdaus, A. T. Hidayat, L. J. Diguna, D. Kowal, A. Bruno, D. Cortecchia, A. Arramel, and M. D. Birowosuto, "Recent developments in low-dimensional heterostructures of halide perovskites and metal chalcogenides as emergent materials: Fundamental, implementation, and outlook," Chem. Phys. Rev. **5**(1), 011303 (2024).

[126]W. Ye, G. Bizarri, M. D. Birowosuto, and L. J. Wong, "Enhancing large-area scintillator detection with photonic crystal cavities," ACS Photonics **9**(12), 3917–3925 (2022).

[127]M. Makowski, W. Ye, D. Kowal, F. Maddalena, S. Mahato, Y. T. Amrillah, W. Zajac, M. E. Witkowski, K. J. Drozdowski, Nathaniel, C. Dang, J. Cybinska, W. Drozdowski, F. A. A. Nugroho, C. Dujardin, L. J. Wong, and M. D.

Birowosuto, "Scaling up Purcell-enhanced self-assembled nanoplasmonic perovskite scintillators into the bulk regime," arxiv:2411.18477 (2024).

[128] Y. Shvyd'ko, S. Stoupin, V. Blank, and S. Terentyev, "Near-100% Bragg reflectivity of X-rays," Nat. Photonics **5**, 539–542 (2011).

[129] E. V. Tkalya, "Decay rate of the nuclear isomer ^{229}Th ($3/2^+$, 7.8 eV) in a dielectric sphere, thin film, and metal cavity," Phys. Rev. Lett. **120**, 122501 (2018).

[130] Y. Zhou, J. Chen, O. M. Bakr, and O. F. Mohammed, "Metal halide perovskites for X-ray imaging scintillators and detectors," ACS Energy Lett. **6**(2), 739–768 (2021).

[131] J. A. Peters, Z. Liu, B. W. Wessels, I. Androulakis, C. P. Sebastian, H. Li, and M. G. Kanatzidis, "Alkali metal chalcogenides for radiation detection," MRS Online Proc. Libr. **1341**, 503 (2011).

[132] X. Li, S. Aftab, S. Hussain, F. Kabir, A. M. A. Henaish, A. G. Al-Sehemi, M. R. Pallavolu, and G. Koyyada, "Dimensional diversity (0D, 1D, 2D, and 3D) in perovskite solar cells: exploring the potential of mixed-dimensional integrations," J. Mater. Chem. A **12**(8), 4421–4440 (2024).

[133] City Labs Inc., "Technology chip graphic," https://citylabs.net/wp-content/uploads/2022/12/technology-chip-graphic.png.webp accessed August 8, 2024.

[134] City Labs Inc., "H_3 betavoltaic power vs time," https://citylabs.net/wp-content/uploads/2023/02/download.png.webp accessed December 17, 2024.

[135] V. A. Tolmachev, T. S. Perova, J. A. Pilyugina, and R. A. Moore, "Experimental evidence of photonic band gap extension for disordered 1D photonic crystals based on Si," Opt. Commun. **259**(1), 104–106 (2006).

[136] D. Chi, S. Lu, R. Xu, K. Liu, D. Cao, L. Wen, Y. Mi, Z. Wang, Y. Lei, S. Qu, and Z. Wang, "Fully understanding the positive roles of plasmonic nanoparticles in ameliorating the efficiency of organic solar cells," Nanoscale **7**(37), 15251–15257 (2015).